Recognition of B-DNA by Neomycin−Hoechst 33258 Conjugates†

Bert Willis‡ and Dev P. Arya*

Laboratory of Medicinal Chemistry, Clemson University, Clemson, South Carolina 29634

Received May 10, 2006; Revised Manuscript Received June 7, 2006

ABSTRACT: Recent developments have indicated that aminoglycoside binding is limited not to RNA but to nucleic acids that, like RNA, adopt conformations similar to the A-form. We have further sought to expand the utility of aminoglycoside binding to B-DNA structures by conjugating neomycin, an aminoglycoside antibiotic, with the B-DNA minor groove binding ligand Hoechst 33258. Described herein are novel neomycin−Hoechst 33258 conjugates developed for exploring B-DNA groove recognition. We have varied the two reported conjugates in linker length and composition in an effort to improve our understanding of the spatial differences that define B-DNA binding. Spectroscopic studies such as ultraviolet (UV) melting, isothermal fluorescence titrations, differential scanning calorimetry (DSC), and circular dichroism (CD) together illustrate the mode of binding by such conjugates. Both conjugates exhibit enhanced thermal stabilization of A·T rich duplexes when compared to Hoechst 33258.

Neomycin is an aminoglycoside antibiotic known for its bactericidal activity (*1*, *2*). The bactericidal effects are believed to result from aminoglycoside binding to the aminoacyl site (A-site) of the 30S subunit of ribosomal RNA. Binding by the aminoglycoside disrupts the fidelity of proper codon−anticodon recognition and results in the incorporation of incorrect amino acid residues within proteins. The end result of these events is enhanced production of proteins of improper function which flood the cell, disrupting cellular function and leading to overall cell death (*1*).

In the past decade, a number of other biologically relevant RNA targets have also been shown to bind aminoglycosides. These include the trans activating region (*3*−*7*), the rev response element (*8*−*12*), and the ψ element (*13*−*15*) of the HIV-1 virus. Ribozymes such as the hepatitis δ (*16*, *17*), hammerhead (*18*−*20*), group I intron (*21*−*23*), and RN*ase* P (*24*−*26*) have also been shown to bind aminoglycosides such as neomycin. Therefore, neomycin represents the aminoglycoside family as a molecule with high affinity for a number of different nucleic acid structures. Recent findings have lengthened the list of nucleic acids to which neomycin is known to bind. Initial studies of aminoglycoside−triplex DNA interactions found neomycin to be the first example of a groove binding ligand that significantly and specifically stabilizes triplex DNA over duplex DNA (*27*−*29*). An enhancement in triplex binding has also been illustrated through the development of neomycin−intercalator conjugates (*30*, *31*). Together with RNA−DNA hybrid studies (*32*) and competition dialysis experiments, it was eventually discovered that aminoglycoside affinity is not restricted to RNA, but instead specific to nucleic acids that are known to adopt the A-form (*33*, *34*).

A-Form conformations are generally adopted under dehydrated conditions. The absence of the spine of hydration lining the minor groove, otherwise present in B-form conformations, renders the phosphate backbone unstable due to charge repulsion. The end result is a wider and shallower minor groove and a deeper and narrower major groove. B-DNA grooves are quite the opposite in width and depth. The structural properties of these different conformations result in a considerable difference in small molecule recognition. B-DNA binding by small molecules has largely been focused in the minor groove. A-Form structures (e.g., RNA duplex) are targeted by major groove binding ligands (e.g., aminoglycosides). The successful targeting of the major groove of B-DNA has been elusive. The design of a ligand that specifically targets the B-DNA (A·T rich oligomers) major groove could inhibit protein interactions necessary for undesirable gene expression.

To date, few carbohydrate interactions with DNA involve interactions within the major groove. Among the classes of compounds known for DNA binding are enediyne antibiotics, anthracyclines, pluramycins, indolocarbazoles, and aureolic acids (*35*). Of the limited number of carbohydrates known and studied for DNA binding, only a select few have displayed major groove contacts. The majority of compounds within this small group are known for dual groove (both minor and major) interactions. These interactions are often assisted by an intercalative structure, assisted by a variety of binding characteristics, as displayed in DNA-cleaving agents (neocarzinostatin), alkylating agents (altromycin B), or tandem intercalative−groove binding ligands (nogalamycin, respinomycin, and NB-506). To this end, it was envisioned that neomycin conjugated to minor groove binders could be used to target B-DNA. A neomycin dimer has previously been suggested to bind in the DNA major groove

† D.P.A. thanks the National Science Foundation (CHE/MCB-0134972) for financial support.

* To whom correspondence should be addressed. E-mail: dparya@clemson.edu. Phone: (864) 656-1106. Fax: (864) 656-6613.

‡ Current address: Scripps Research Institute, La Jolla, CA 92037.

10.1021/bi0609265 CCC: $33.50
Published on Web 08/04/2006

with high affinities (*35*, *36*). To investigate the effect of binding of neomycin to B-DNA, we have covalently linked neomycin with Hoechst 33258, a well-known minor groove binding ligand with particular affinity for A·T bases known to adopt B-form structures. Conjugates of Hoechst with other DNA-binding moieties have indicated enhancements in recognition over Hoechst 33258 alone. These include conjugates with porphyrins (*37*, *38*), polyamides (*39*, *40*), polyamines (*41*, *42*), and DNA (*43*−*46*). Reported herein are the design, synthesis, and spectroscopic studies of novel neomycin−Hoechst 33258 conjugates designed and studied for recognition of B-DNA. The results illustrate the preliminary successes in extending aminoglycoside recognition to include the major groove of B-DNA.

MATERIALS AND METHODS

Nucleic Acids

DNA polymers were purchased from Pharmacia Biotech (Piscataway, NJ). Concentrations were determined by UV absorbance using an ϵ_{260} of 6000 M^{-1} cm^{-1} for poly(dA)·poly(dT) and an ϵ_{264} of 8520 M^{-1} cm^{-1} for poly(dT). DNA oligomers $d(A)_{22}$, $d(T)_{22}$, d(CGCAAATTTGCG), and d(CGCAAGCTTGCG) were purchased from Integrated DNA Technologies (Coralville, IA) and quantitated using extinction coefficients provided by the supplier. Oligomer duplex formation was accomplished by slowly annealing from 95 °C (0.2 °C/min). The buffer used for polymeric DNA consisted of 10 mM sodium cacodylate, 0.5 mM EDTA, and 150 mM KCl (pH 7.2). For $d(A)_{22}$ and $d(T)_{22}$, the buffer was identical to polymeric DNA except a pH of 6.8 was used. Experiments with the self-complementary 12mer were carried out in BPES buffer [6 mM Na_2HPO_4, 2 mM NaH_2PO_4, 1 mM EDTA, and 185 mM NaCl (pH 7.0)].

Chemicals

Neomycin B (sulfate salt) was purchased from ICN Biomedicals and used without further purification. Sodium cacodylate, NaCl, and sodium phosphate salt were purchased from Fisher Scientific. Hoechst 33258 was purchased from Acros Organics. Conjugate NH1 was synthesized as reported previously (*43*). Quantitation of Hoechst 33258 (ϵ_{338} = 42 000 M^{-1} cm^{-1}) and NH1 (ϵ_{342} = 39 241 M^{-1} cm^{-1}) in aqueous solutions was carried out using UV absorbance. To ensure the stability and minimum adsorption of Hoechst compounds to container walls, all solutions were stored in nontransparent, polystyrene tubes. Diisopropylazodicarboxylate (DIAD) and 1,1′-thiocarbonyldi-2(1*H*)-pyridone (TCDP) were purchased from Aldrich Chemical Co.; all other reagents were purchased from Acros Organics and used without further purification. All solvents were purchased from VWR. Reaction solvents were distilled over calcium hydride (pyridine, dichloromethane, and DMF) or sodium metal [diethyl ether, dioxane, and ethanol (EtOH)]. Dry EtOH for imidate formation was distilled first with sodium metal, with further distillation over magnesium pellets.

Methods

UV Melting. All experiments were carried out using a Cary 100E UV−vis spectrophotometer equipped with a thermoelectrically controlled 12-cell holder. All samples were analyzed in quartz cells (1 cm path length). Lamp stability and wavelength alignment were checked prior to each experiment. Concentrations of DNA were 15 μM for poly(dA)·2poly(dT) and 1 μM (in duplex) for all oligomers. Ligand concentrations varied and are stated in the figure legends. Samples were prepared by heating the DNA/ligand mixtures (in polystyrene tubes) to 95 °C, keeping them at 95 °C for 5 min, and slowly cooling them to room temperature before incubation at 4 °C for 16 h before UV analysis at 260 nm with heating ramped from 20 to 95 °C at 0.2 °C/min.

Fluorescence Titrations. Equilibrium binding experiments were carried out using a Photon Technology International (Lawrenceville, NJ) instrument at ambient temperature (22 °C). A solution of ligand (serially diluted to working concentrations) was excited at its respective λ_{max} (slits of 2 or 4 nm), and resulting emission curves (from 390 to 600 nm) were recorded after serial additions of a concentrated DNA solution [that of poly(dA)·poly(dT) was 200 μM/base]. After each addition, the solution was mixed by pipetting up and down with a Pasteur pipet treated with silanizing agent (Sigmacote) to prevent adsorption of ligand to the glass. Sample equilibrium was monitored by continually exciting and/or scanning the sample at different times and was usually reached within 2 min. All data were normalized to account for the (small) dilution of the sample upon addition of substrate. For the self-complementary 12mer experiments, individual samples with varying ligand:DNA ratios were prepared, all with a constant ligand concentration of 100 nM. A silanized (SigmaCote) or polystyrene cuvette was used in all experiments. Corresponding fluorescence data were fit using Kaleidagraph according to eq 1:

$$F_0 + [(F_b - F_0)/(2C_T)]\{[DNA]/N + C_T + 1/K_b - [([DNA]/N + C_T + 1/K_b)^2 - 4[DNA]/N \times C_T]^{1/2}\} \quad (1)$$

where F_0 is fluorescence of the ligand in the absence of DNA, F_b is the fluorescence of the fully bound ligand, C_T is the total ligand concentration, K_b is the binding constant, N is the binding site size, and [DNA] is the DNA concentration at each titration. Values for F_0, F_b, and K_b can be determined by curve fitting a plot of fluorescence versus DNA concentration. Binding site size N can be determined by mixing curve analysis (Job plots) or by titrations of a constant DNA concentration with concentrated ligand to determine the number of base pairs per ligand, n, at relatively high concentrations (5 μM DNA with a ligand concentrations of up to 5 μM) (*44*). When fit to the theoretical independent site model, the values of DNA (in base pairs) can be divided by N, represented as the number of identical base pairs containing a single binding site, to provide values for binding site concentration. For Hoechst 33258, an N value of 10 was used in accordance with the literature (*45*−*47*). Since Hoechst 33258 has been shown to target six A·T base stretches, an N value of 10 was used since it has been shown that $N = 2(n - 1)$, where n equals the number of base pairs bound by ligand (*48*).

CD Spectropolarimetry Titrations. CD experiments were carried out at 20 °C using a Jasco J-810 spectropolarimeter. A concentrated solution of ligand (200 μM) was added to a 30 μM solution of poly(dA)·poly(dT) and allowed to stir constantly before being scanned from 450 to 210 nm. As

with fluorescence experiments, equilibrium was determined by periodically scanning the sample over a 10 min period for the first few additions of ligand and was reached within 3 min. An average of three scans was gathered for each titration point. All data were normalized to account for the (small) dilution of sample upon addition of ligand.

Differential Scanning Calorimetry. DSC experiments were carried out on a MicroCal VP-DSC instrument. Samples of DNA (512 μL of a 100 μM/bp solution) in the absence and presence of ligand (8 μM) were heated from 20 to 110 °C at a scan rate of 30 °C/h. After buffer subtraction (usually negligible), baseline adjustments, T_m assignments, and peak integrations were carried out using instrument software (Origin 5.0). Values for ΔH at the T_m were determined by dividing the integrated values by the cell volume and DNA concentration. Values of duplex melting (no ligand) can be designated as ΔH_1, and values for both duplex and ligand dissociation can be represented as ΔH_2. Both can be used in determining the enthalpy of ligand binding according to the equation

$$\Delta H_b = -\left(\frac{\Delta H_2 - \Delta H_1}{r_{db}}\right) \quad (2)$$

where ΔH_b corresponds to the enthalpy of ligand binding and r_{db} is the ratio of ligand concentration to base pair concentration. The value for ΔH_b can be used to determine the binding constant at any temperature T (kelvin) according to the standard van't Hoff equation:

$$\ln\frac{K}{K_{T_m}} = -\left(\frac{\Delta H_b}{R}\right)\left(\frac{1}{T} - \frac{1}{T_m}\right) \quad (3)$$

where K represents the binding constant at temperature T, T_m is the melting temperature of the DNA−ligand complex, determined using either UV or DSC, and R is the gas constant. The value of K_{T_m}, the binding constant at T_m, is determined using eq 4:

$$\frac{1}{T_m^\circ} - \frac{1}{T_m} = \left(\frac{R}{\Delta H_m}\right)\ln(1 + K_{T_m}L)^{1/n} \quad (4)$$

where T_m° and T_m are represented by duplex melting alone and in the presence of ligand, respectively. The value for ΔH_m equals ΔH_1, simply the ΔH of duplex melting alone. The value for n represents the binding stoichiometry, which can be determined using fluorescence titrations (Figure 11). The method of using DSC for determining binding constant data is in accordance with that reported previously (*49*).

Viscometry. Viscosity measurements were conducted using a Cannon-Ubbelohde 75 capillary viscometer submerged in a water bath at 27 ± 0.05 °C. Flow times of buffer only followed by DNA (1030 μL of 100 μM in base pairs) were recorded in triplicate before titrations of concentrated ligand solutions (500 μM) with mixing by bubbling of air through the solution. Flow times after each titration were recorded in triplicate. In all cases, standard deviations were less than 0.1 s. Flow times for ligand titrations into DNA ranged from 110 to 108 s. DNA solutions were in 10 mM sodium cacodylate buffer containing 150 mM KCl and 1 mM $MgCl_2$ (pH 7.2). Data analysis for each experiment was carried out as reported previously. (*29*).

Computer Modeling. The DNA duplex d(CGCAAATTTGCG)$_2$ was extracted from PDB entry 296d (*50*). Conformational optimization of neomycin, docked closest to its 5′ position with respect to the Hoechst linker, was carried out prior to attachment to Hoechst using a Monte Carlo routine in MacroModel, using the AMBER* force field and water as solvent, as reported previously (*29*). The continuum GB/SA model of water, as implemented in MacroModel, was used in all calculations. Five of the six amines in neomycin were protonated, in agreement with NMR studies of neomycin (*51*, *52*), as well as the terminal amine in the piperazine ring of the Hoechst moiety.

*Synthesis of Compounds **2**−**10***

*4-{2-[2-(2-{2-[2-(2-Hydroxyethoxy)ethoxy]ethoxy}ethoxy)-ethoxy]ethoxy}benzonitrile (**2**).* To a solution of hexaethylene glycol **1** (1.0 g, 3.5 mmol), *p*-cyanophenol (210 mg, 1.8 mmol), and triphenylphosphine (928 mg, 3.5 mmol) in dioxane (30 mL) was added DIAD (0.7 mL, 3.5 mmol) dropwise at 0 °C over a period of 30 min with vigorous stirring (heterogeneous mixture). The dioxane was evaporated after the solution had reached room temperature and been stirred overnight. The residue was dissolved in ethyl acetate (50 mL) and washed with 5% $NaHCO_3$ (30 mL) and water (30 mL). The organic layer was dried with Na_2SO_4 before solvent removal and purification of the oil via column chromatography (gradient of 0 to 10% MeOH in EtOAc). Yield: 345 mg (51%). R_f = 0.26 (9:1 EtOAc/MeOH). ^{1}H NMR (300 MHz, $CDCl_3$): δ 7.59 (d, 2H, J = 7.1 Hz), 6.99 (d, 2H, J = 7.1 Hz), 4.18 (t, 2H, J = 4.7 Hz), 3.87 (t, 2H, J = 4.8 Hz), 3.74−3.59 (m, 20H). ^{13}C NMR (75 MHz, $CDCl_3$): δ 162.0, 134.0, 119.0, 116.0, 104.0, 73.0, 71.1(2), 70.8, 70.1, 69.6, 68.0, 62.0. MALDI-TOF: calcd for $C_{19}H_{29}NO_7$ $[M]^+$ 383.44, found 383.02.

*Toluene-4-sulfonic Acid 2-{[(Ethoxy)ethoxy]ethoxy}ethyl Ester (**3**).* To a solution of **2** (226 mg, 0.59 mmol) in 20 mL of dry CH_2Cl_2 were added *p*-toluenesulfonyl chloride (327 mg, 1.7 mmol) and Et_3N (171 mg, 1.7 mmol) at 0 °C under a N_2 atmosphere, and the mixture was allowed to gradually come to room temperature with overnight stirring. The resulting solution was concentrated to a residue, dissolved in CH_2Cl_2 (30 mL), and washed with dilute citric acid (2 × 10 mL). The organic layer was then dried over anhydrous Na_2SO_4 and evaporated before chromatography (30 to 0% hexane in EtOAc and then 0 to 10% MeOH in EtOAc) afforded 206 mg of **3** (72%) as the pure product. Starting material (**3**, 21 mg) was also recovered. R_f = 0.43 (EtOAc). ^{1}H NMR (300 MHz, $CDCl_3$): δ 7.80 (d, 2H, J = 8.0 Hz), 7.58 (d, 2H, J = 8.8 Hz), 7.35, (d, 2H, J = 8.0 Hz), 6.98 (d, 2H, J = 8.8 Hz), 4.17−4.14 (m, 4H), 3.87 (t, 2H, J = 4.6 Hz), 3.70−3.58 (m, 18H), 2.44 (s, 3H). ^{13}C NMR (75 MHz, $CDCl_3$): δ 146.0, 134.0, 130.0, 128.0, 120.0, 116.0, 71.0 (m), 70.1, 69.5(2), 69.8, 68.0, 22.0. MALDI-TOF: calcd for $C_{26}H_{35}NO_9S$ $[M + H]^+$ 538.62, found 538.34.

*4-{2-[2-(2-{2-[2-(2-Azidoethoxy)ethoxy]ethoxy}ethoxy)-ethoxy]ethoxy}benzonitrile (**4**).* To a solution of compound **3** (206 mg, 0.38 mmol) in DMF (5 mL) containing 3 Å molecular sieves were added NaN_3 (128 mg, 1.97 mmol) and KI (16 mg, 0.09 mmol). The resulting solution was heated at 70 °C for 4 h under argon. TLC indicated product formation upon ninhydrin staining (product is light yellow-

brown; starting tosylate is a faint white color upon staining). Product and starting tosylate have identical R_f values (1% MeOH in CH_2Cl_2). DMF was removed under high vacuum (50 °C), and the residue was dissolved in CH_2Cl_2 (50 mL), washed with water (2 × 25 mL) followed by brine (25 mL), and dried over anhydrous Na_2SO_4. After sufficient solvent removal, the crude mixture was purified over a column of silica (0 to 3% MeOH in CH_2Cl_2) to give 133 mg (86%) of product. R_f = 0.56 (97:3 CH_2Cl_2/MeOH). ^{1}H NMR (300 MHz, $CDCl_3$): δ 7.59 (d, 2H, J = 8.8 Hz), 6.99 (d, 2H, J = 8.8 Hz), 4.17−4.14 (t, 2H, J = 4.7 Hz), 3.88 (t, 2H, J = 4.7 Hz), 3.72−3.66 (m, 18H), 3.39 (t, 2H, J = 5.0 Hz). ^{13}C NMR (75 MHz, $CDCl_3$): δ 163.0, 134.0, 119.0, 115.0, 105.0, 71.6 (m), 70.0 (2), 69.0, 68.0, 51.0. MALDI-TOF: calcd for $C_{19}H_{28}N_4O_6$ $[M]^+$ 408.45, found 408.26.

*N-(2-{2-[2-(2-{2-[2-(4-Cyanophenoxy)ethoxy]ethoxy}-ethoxy)ethoxy]ethoxy}ethyl)-2,2,2-trifluoroacetamide (**5**).* To a solution of compound **4** (133 mg, 0.33 mmol) in EtOH (20 mL) was added 20 mg of 10% Pd/C. The solution was reduced on a Parr shaker using H_2 (45 psi, 10 h). The Pd/C was filtered using Celite and rinsed liberally with EtOH. The EtOH was removed, and the resulting amine intermediate was dried under high vacuum to give 84 mg (68%) which was immediately used without characterization.

To the amine (84 mg, 0.22 mmol) were added MeOH (5 mL) and triethylamine (129 mg, 1.3 mmol). The resulting solution was allowed to stir at 0 °C before dropwise additions of trifluoroacetic anhydride (180 μL, 1.3 mmol) over a period of 20 min. The solution was allowed to come to room temperature with overnight stirring. TLC indicated product formation, though consumption of starting amine was incomplete. Nonetheless, the solution was concentrated and taken up in EtOAc (30 mL) before being washed with dilute citric acid (2 × 20 mL), water (20 mL), and brine (20 mL) and dried over Na_2SO_4. Chromatography (30 to 0% hexane in EtOAc) afforded 33 mg of product. Starting amine (45 mg) was recovered after neutralization of the acid layer and extraction into methylene chloride to give an overall quantitative yield. R_f = 0.42 (EtOAc). ^{1}H NMR (300 MHz, $CDCl_3$): δ 8.0 (br s, 1H, N*H*COCF$_3$), 7.59 (d, 2H, J = 8.8 Hz), 6.98 (d, 2H, J = 8.8 Hz), 4.17 (t, 2H, J = 4.6 Hz), 3.88−3.53 (m, 22H). ^{13}C NMR (75 MHz, $CDCl_3$): δ 162.0, 134.0, 132.0, 130.0, 119.0, 115.0, 104.0, 71.6 (m), 70.6, 69.1, 68.0, 40.0. MALDI-TOF: calcd for $C_{21}H_{29}F_3N_2O_7$ $[M]^+$ 478.46, found 478.40.

*2,2,2-Trifluoro-N-{2-[2-(2-{2-[2-(2-{4-[5-(4-methylpiperazin-1-yl)-1H,1′H[2,5′]-bibenzoimidazolyl-2′-yl]phenoxy}-ethoxy)ethoxy]ethoxy}ethoxy)ethoxy]ethyl}acetamide (**7**).* Compound **5** was converted into the corresponding imidate ethyl ester by vigorously bubbling anhydrous HCl into a solution of **5** in dry EtOH for 30 min before storage at 4 °C overnight. After acid removal (bubbling nitrogen through the solution into a saturated $NaHCO_3$ solution) and EtOH evaporation, imidate **6** was rinsed with dry ether before evaporation and then immediately used without characterization.

To a solution of imidate **6** (33 mg, 59 μmol) in glacial acetic acid (2 mL) was added 2-(3,4-diaminophenyl)-6-(1-methyl-4-piperazinyl)benzimidazole (19 mg, 59 μmol) before it was refluxed for 8 h under argon. The acetic acid was removed, and the crude mixture was loaded onto a column of silica and purified using a gradient of MeOH (0 to 15%) in CH_2Cl_2 containing trace NEt_3. Evaporation of the solvent and washing with ether afforded 9 mg of **7** (20%) of an orange-yellow solid. R_f = 0.29 (85:15:0.1 CH_2Cl_2/MeOH/NEt_3). ^{1}H NMR (300 MHz, $CDCl_3$): δ 8.25 (s, 1H), 8.05 (d, 2H, J = 8.7 Hz), 7.93 (d, 1H, J = 8.8 Hz), 7.69 (d, 1H, J = 8.8 Hz), 7.51 (d, 1H, J = 8.7 Hz), 7.11−7.02 (m, 4H), 4.24−4.14 (m, 2H), 3.90−3.80 (m, 2H), 3.69−3.54 (m, 18H), 3.50−3.40 (m, 2H), 3.30−3.20 (m, 4H), 2.75−2.60 (m, 4H), 2.37 (s, 3H). MS MALDI-TOF: calcd for $C_{39}H_{48}F_3N_7O_7$ $[M]^+$ 783.84, found 783.58.

*Boc-Protected Neomycin−HEG−Hoechst 33258 Conjugate NH2 (**9**).* To a solution of **7** (9 mg) in a 2:1 MeOH/H_2O mixture (1.5 mL) was added K_2CO_3 (7 mg), and the resulting solution was stirred overnight at room temperature. Solvent removal and coevaporation with dry pyridine (2 × 3 mL) gave compound **8** which was redissolved in dry pyridine (2.5 mL). Addition of **8** to neomycin isothiocyanate (20 mg, 15.2 μmol) and DMAP (1 mg) was carried out without characterization. The solution containing amine, neomycin isothiocyanate, DMAP, and pyridine was allowed to stir at room temperature under argon for 20 h. After pyridine was removed in vacuo, the residue was purified via column chromatography (0 to 20% MeOH in CH_2Cl_2) to yield 12 mg of **9** (52%). R_f = 0.65 (85:15:0.1 CH_2Cl_2/MeOH/NEt_3). ^{1}H NMR (500 MHz, $CDCl_3$): δ 8.27 (s, 1H), 8.09 (d, 2H, J = 8.7 Hz), 7.95 (d, 1H, J = 8.8 Hz), 7.71 (d, 1H, J = 8.8 Hz), 7.53 (d, 1H, J = 8.7 Hz), 7.27−7.16 (m, 4H), 7.14 (d, 2H), 7.09 (d, 1H), 6.93 (br s, 1H), 6.57 (br s, 1H), 6.51 (br s, 1H), 5.40 (br s, 1H), 5.13 (br s, 1H), 4.27−4.22 (m, 2H), 4.09 (br s, 1H), 3.90−3.20 (m, 43H), 2.92−2.80 (m, 6H), 2.52 (s, 3H), 1.44−1.42 (m, 54H). MALDI-TOF: calcd for $C_{93}H_{146}N_{14}O_{30}S_2$ $[M]^+$ 2004.36, found 2004.25.

*Neomycin−HEG−Hoechst 33258 Conjugate NH2 (**10**).* To a solution of **9** (3 mg, 1.5 μmol) in dry CH_2Cl_2 (1 mL) and 51 μL of ethanedithiol was added trifluoroacetic acid (1 mL) before the mixture was stirred at room temperature for 3 h. The solution was concentrated followed by the addition of ether to give a light brown solid which, after subsequent washing with ether and drying under vacuum, was dissolved in deionized water and lyophilized to afford 3.4 mg of **10** (94%). The purity of the product was checked by analytical HPLC (Supelcosil LC18S column; eluent of aqueous 0.1% TFA with a gradient from 0 to 100% of a 95:5 acetonitrile/water mixture over a period of 20 min; flow rate of 1.2 mL/min; ambient temperature; retention time of product of 8.1 min; see the Supporting Information). UV (H_2O): λ_{max} = 342 nm, ϵ = 21 085 M^{-1} cm^{-1}. ^{1}H NMR (500 MHz, $CDCl_3$): δ 8.78 (d, 2H, J = 6.9 Hz), 8.61 (s, 1H), 7.80−8.10 (m, 4H), 7.70 (s, 1H), 7.32 (s, 2H), 7.20 (br s, 1H), 6.86 (s, 1H), 6.08 (s, 1H), 5.41 (s, 1H), 5.30 (s, 1H), 2.69−4.00 (m, 55H). MALDI-TOF: calcd for $C_{63}H_{98}N_{14}O_{18}S_2$ $[M]^+$ 1403.67, found 1403.30.

Synthesis of NH1 compounds **12** and **13** has been reported previously (*47*).

RESULTS AND DISCUSSION

Design of Neomycin−Hoechst 33258 Conjugates. Hoechst 33258 was chosen as the minor groove binder for conjugation with neomycin for three primary reasons. (a) Hoechst compounds significantly fluoresce upon sequence-specific DNA binding, allowing for equilibrium binding studies at low (nanomolar) concentrations. (b) Synthetic modification

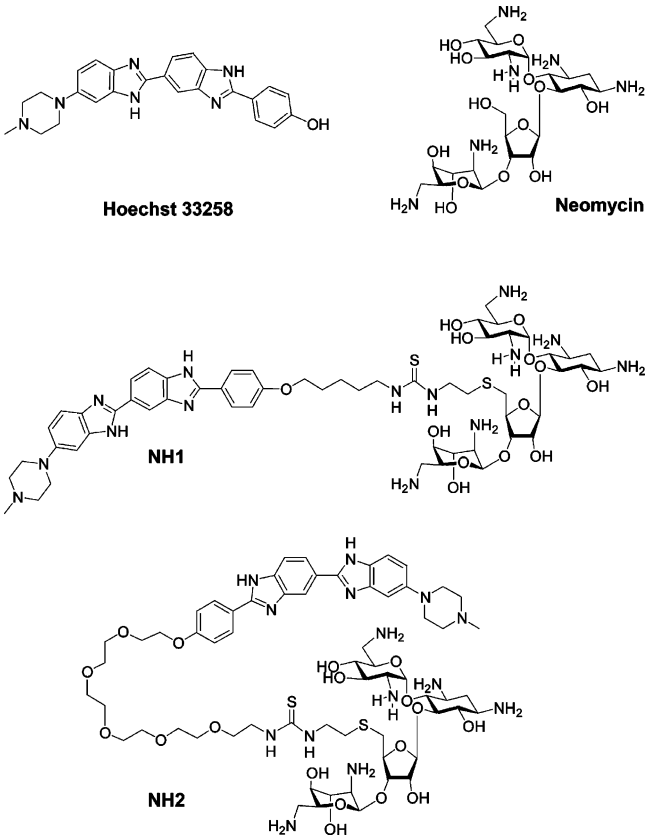

FIGURE 1: Structures of Hoechst 33258, neomycin, and conjugates NH1 and NH2.

at the terminal phenol is easy. Other minor groove-binding ligands lack this combination. For example, the fluorescence of polyamides is significantly lower, and changes in fluorescence upon DNA binding are not significant. Fluorescence assays often involve competitive experiments with Hoechst compounds to monitor changes in the Hoechst signal (*39*). Ligands that do significantly fluoresce either lack terminal positions for straightforward chemical modification or are intercalators lacking sequence specificity. (c) Hoechst 33258 binds to duplex DNA with very high affinity (10^8 M^{-1}), whereas neomycin shows no binding to A·T rich DNA duplexes at physiological salt concentrations ($<10^3$ M^{-1}). Thus, forcing a molecule such as neomycin into the major groove can have a negative effect on Hoechst binding in the DNA minor groove. Hoechst's high affinity allows determination of these effects quantitatively as long as the decrease in the level of binding is less than 3−4 orders of magnitude.

Two extremes were explored in determining the linker between Hoechst 33258 and neomycin. One involved a short linker with minimal number of atoms between the two binding moieties, while the other involved a longer and more flexible linkage. Figure 1 shows the structures of two conjugates (NH1 and NH2). Both choices were examined using molecular modeling (MacroModel) with d(CGCAAATTTGCG)$_2$. For the short linker, it was found that a pentane moiety separating the two reactive positions (of Hoechst and neomycin) gave the optimum binding without significant departure of either binding moiety from its respective groove (Figure 2, left). In investigating the longer length, we chose a hexaethylene glycol linker (Figure 2, right). Even though there is a considerable area separating

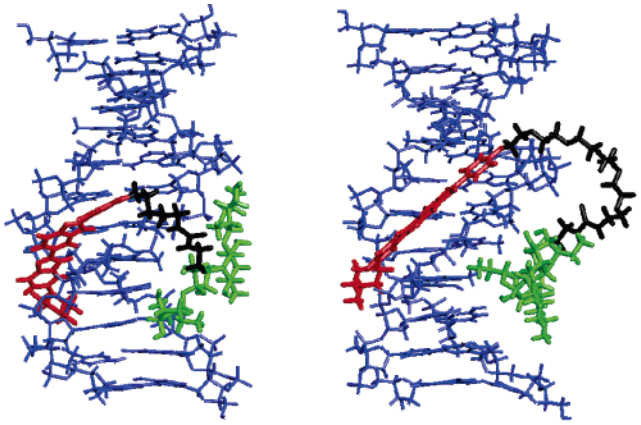

FIGURE 2: Computer model of NH1 (left) and NH2 (right) binding to d(CGCAAATTTGCG)$_2$. The Hoechst region is colored red, neomycin green, and the hexaethylene glycol linker black. DNA is colored blue.

Scheme 1[a]

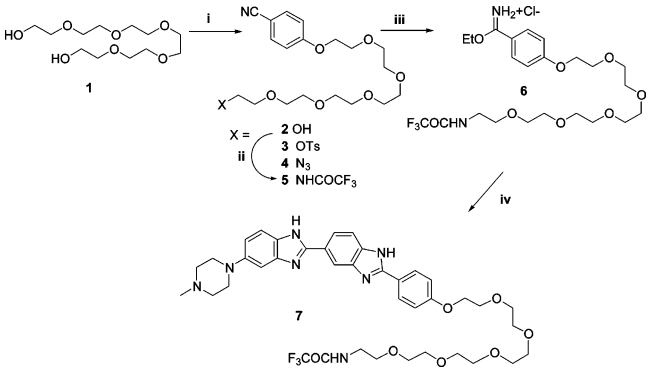

[a] Reagents and conditions: (i) *p*-cyanophenol, PPh_3, DIAD, dioxane, 51%; (ii) (a) TsCl, CH_2Cl_2, NEt_3, 72%; (b) NaN_3, DMF, NaI, 86%; (c) H_2, 10% Pd/C, EtOH, 68%; (d) trifluoroacetic anhydride, CH_2Cl_2, pyridine, quantitative; (iii) HCl(g), EtOH, quantitative; (iv) 2-(3,4-diaminophenyl)-6-(1-methyl-4-piperazinyl)benzimidazole, HOAc, 20%.

the linker from both neomycin and Hoechst, binding of these two molecules remained intact. Linkers longer than hexaethylene glycol induced considerable separation of neomycin from the major groove. The linker precursors to the synthesis of these two conjugates were commercially available, reducing the number of synthetic steps. Last, the choice in linkers provides a striking contrast when comparing length and flexibility. Such comparison would prove to be insightful in determining the importance of linkers in developing dual-binding ligands.

Synthesis of NH1 and NH2. Scheme 1 details the reaction scheme for the preparation of the Hoechst−HEG-amine derivative. A Mitsunobu reaction of hexaethylene glycol **(1)** with *p*-cyanophenol was carried out according to a reported procedure (*45*). Tosylation of the terminal hydroxyl, followed by azide substitution with subsequent reduction, afforded the terminal amine, which was protected as a trifluoracetamide before imidation and coupling. The imidate ester **(6)** was successfully coupled with 2-(3,4-diaminophenyl)-6-(1-methyl-4-piperazinyl)benzimidazole to give the desired Hoechst−linker component **(7)** necessary for conjugation with neomycin. Deprotection and reaction with neomycin isothiocyanate (Neo-NCS, Scheme 2) were carried out in a fashion similar to previous reports (*48*). NH1 and NH2 were obtained by coupling of Neo-NCS to Hoechst amines **11** and **8**,

Scheme 2[a]

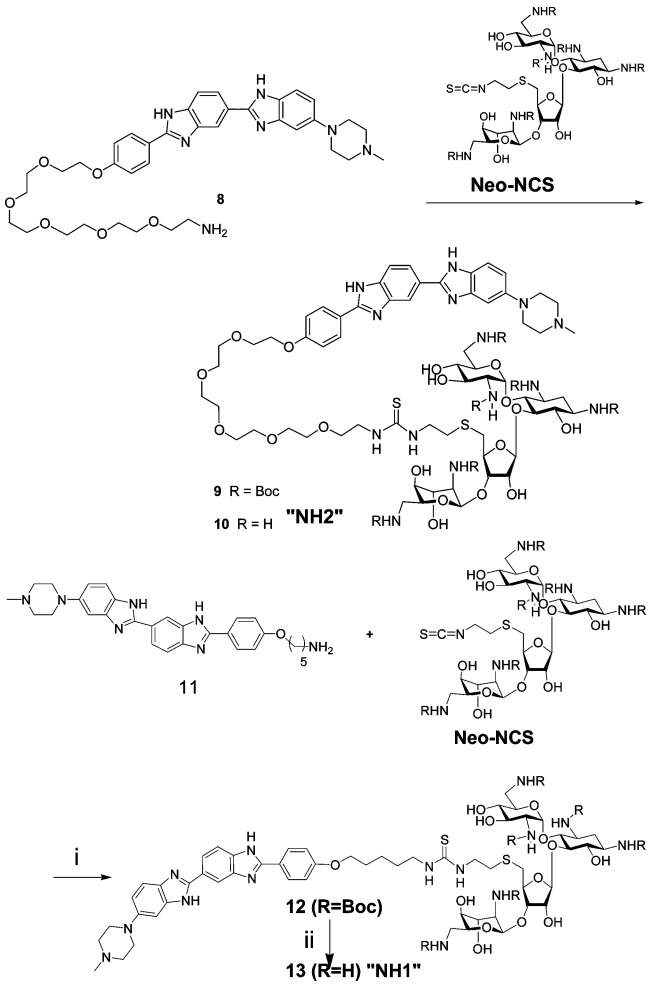

[a] Reagents and conditions: (i) pyridine, DMAP, 52%; (ii) 1:1 TFA/CH_2Cl_2 mixture, 94%.

respectively, followed by deprotection with TFA (Scheme 2).

The NH1 Conjugate Significantly Increases the Thermal Stability of Poly(dA)·Poly(dT) over NH2. Due to neomycin's significant enhancement on triplex DNA stability, UV melting studies with poly(dA)·2poly(dT) were first carried out in an effort to analyze NH1 and NH2 binding. When mixed in a 2:1 ratio under appropriate salt conditions, poly(dT) can associate with poly(dA) to form a poly(dA)·2poly(dT) triplex. Dissociation of the third poly(dT) strand from the poly(dA)·poly(dT) duplex can be monitored with slow heating of the DNA sample accompanying UV absorbance measurements at 260 nm. The "melting" of the triplex to duplex and single strand is represented by a hyperchromic transition in the absorbance versus temperature profile. A more pronounced transition at higher temperatures corresponds to duplex dissociation. Using first-derivative analysis in the UV−vis software provides the melting temperature (T_m), which represents the temperature at which the helix is half-dissociated. Samples of nucleic acid in the presence of ligand may display shifts in T_m values, indicating a destabilization (lower T_m than in the absence of ligand) or stabilization (higher T_m than in the absence of ligand).

As Figure 3 shows, substantial differences between NH1 and NH2 are apparent. Given that Hoechst 33258 alone

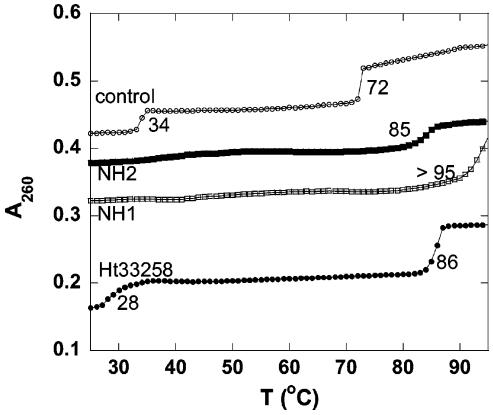

FIGURE 3: UV melting profiles of poly(dA)·2poly(dT) with NH1 and NH2. Samples of DNA (15 μM/bp) were mixed with ligand (2 μM) in buffer [10 mM sodium cacodylate, 0.5 mM EDTA, and 150 mM KCl (pH 7.2)] before being heated at 95 °C for 5 min and slowly annealed to 20 °C before UV analysis at 260 nm from 20 to 95 °C at a heating rate of 0.2 °C/min.

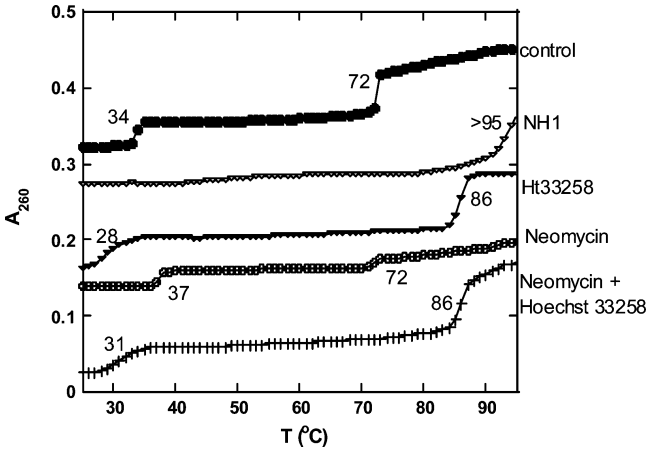

FIGURE 4: UV melting profiles of poly(dA)·2poly(dT) with various ligands. Samples of DNA (15 μM) were mixed with ligand (2 μM) in buffer [10 mM sodium cacodylate, 0.5 mM EDTA, and 150 mM KCl (pH 7.2)] before being heated at 95 °C for 5 min and slowly annealed to 20 °C before UV analysis at 260 nm from 20 to 95 °C at a heating rate of 0.2 °C/min.

significantly stabilizes poly(dA)·poly(dT) and neomycin shows poor binding to duplex DNA structures, it is safe to assume that the Hoechst moiety in the conjugates drives the binding to DNA. In fact, a slight decrease in T_m was observed with NH2 (Figure 3) when compared to that of Hoechst 33258 (Figure 4). This decrease suggests the entropic penalty from the longer and more flexible linker diminishes the tandem binding contributions of each moiety. Alternatively, NH1, possessing a shorter, alkyl linker, that docks neomycin in the proximity within the major groove backbone greatly shifts the T_m when compared to Hoechst 33258 (>11 °C).

NH1 Inhibits Triplex DNA Formation and Significantly Stabilizes Duplex DNA Compared to Hoechst 33258. The thermal stability of poly(dA)·2poly(dT) in the presence of neomycin, Hoechst 33258, and NH1 was further investigated. It was found that the conjugate displays a marked effect on the stability of the poly(dA)·poly(dT) duplex when compared to both neomycin (which is known to have no effect on the thermal stability of duplex DNA) and Hoechst 33258. As depicted in Figure 4, the dissociation of duplex DNA in the presence of NH1 occurs at a temperature (>95 °C) higher than that of DNA in the presence of Hoechst 33258 (86 °C)

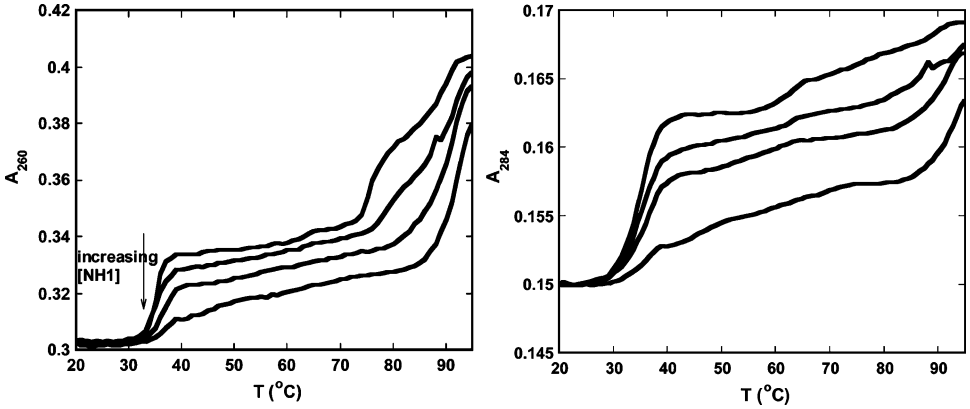

FIGURE 5: UV melting profiles of poly(dA)·2poly(dT) with NH1. Samples of poly(dA)·2poly(dT) (15 μM) were mixed with ligand (from 0.5 to 1.25 μM) in buffer [10 mM sodium cacodylate, 0.5 mM EDTA, and 150 mM KCl (pH 7.2)] before being heated at 95 °C for 5 min and slowly annealed to 20 °C before UV analysis at 260 and 284 nm from 20 to 95 °C at a heating rate of 0.2 °C/min. The curves shown are for the DNA triplex in the presence of 0.5, 0.75, 1.0, and 1.25 μM NH1, monitored at 260 (left) and 284 nm (right).

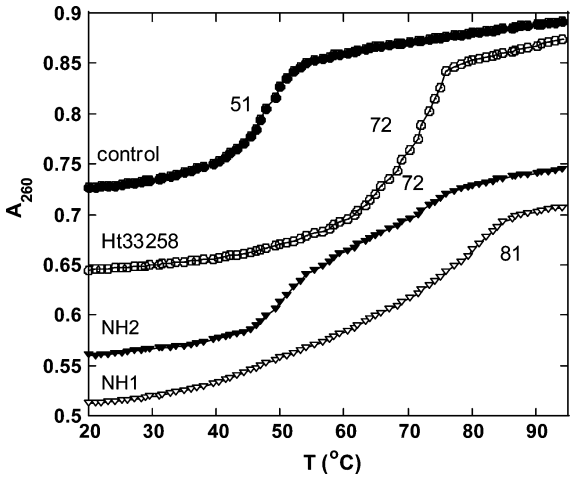

FIGURE 6: UV melting profiles of $d(A)_{22}$·$d(T)_{22}$ with various ligands. Samples of DNA (1 μM in duplex) were mixed with ligand (3 μM) in buffer [10 mM sodium cacodylate, 0.5 mM EDTA, and 150 mM KCl (pH 6.8)] before being heated at 95 °C for 5 min and slowly annealed to 20 °C before UV analysis at 260 nm from 20 to 95 °C at a heating rate of 0.2 °C/min.

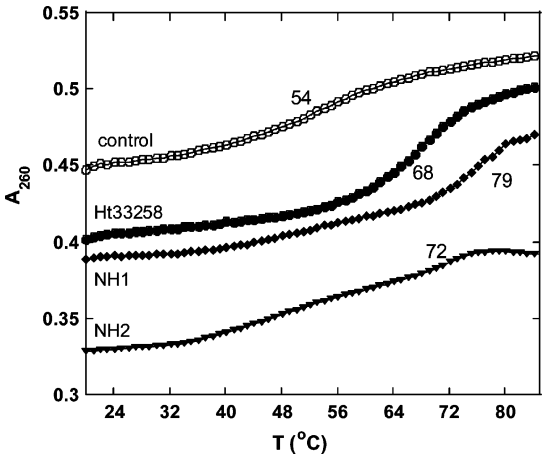

FIGURE 7: UV melting profiles of $d(CGCAAATTTGCG)_2$ with various ligands. Samples of DNA (1 μM in duplex) were mixed with ligand (1 μM) in BPES buffer [6 mM Na_2HPO_4, 2 mM NaH_2PO_4, 1 mM EDTA, and 185 mM NaCl (pH 7.0)] before being heated at 95 °C for 5 min and slowly annealed to 20 °C before UV analysis at 260 nm from 20 to 95 °C at a heating rate of 0.2 °C/min.

and neomycin (72 °C, unchanged when compared to native duplex melting), suggesting that the interaction between NH1 is stronger than those between the individual parent compounds. Samples containing both neomycin and Hoechst 33258 displayed no difference in T_m from that observed with the individual molecules. It is important to note that clear triplex melting was not observed for poly(dA)·2poly(dT) in the presence of the conjugate NH1 under these conditions (2 μM ligand). This suggests that duplex binding of the drug prevents the third strand polypyrimidine from binding in the major groove. Further support of neomycin binding in the major groove was found in a concentration-dependent melting study with NH1, in which the triplex melting transition is seen to gradually disappear (Figure 5). At 284 nm, where triplex transitions are clearly visible, a similar effect is seen. These results strongly support the design of dual groove binding, where Hoechst 33258 rests in the minor groove while the tethered neomycin region docks within the major groove. NH2 also exhibited diminished triplex melting profiles, indicating a major groove binding and a blockage of third strand binding to the duplex upon sample preparation (slow annealing from 95 °C, data not shown).

The NH1 Conjugate Significantly Increases the Thermal Stability of Shorter DNA Duplexes. To test the effect of the conjugates on oligomeric DNA duplex stability, UV melting profiles of $d(A)_{22}$·$d(T)_{22}$ in the absence and presence of various ligands (Figure 6) were gathered in a manner similar to that of polymeric DNA. An effect analogous to that of poly(dA)·poly(dT) was observed. Melting of $d(A)_{22}$·$d(T)_{22}$ alone gives a T_m of 51 °C, whereas in the presence of Hoechst 33258, the duplex transition occurs at 72 °C (ΔT_m = 21 °C). Samples containing NH1 under similar conditions exhibited a significant shift in T_m (81 °C, ΔT_m = 31 °C). For NH2, a T_m of 72 °C was observed, suggesting no real influence of neomycin on the stabilization of the DNA. This observation is a good indication that increased linker length and flexibility can be detrimental to strong, dual groove binding. Also, the melting profile under these conditions (1 μM duplex^{-1} DNA, 3 μM ligand) for NH2 and NH1 was biphasic; a transition at 51 °C was observed, signifying the melting of unbound DNA.

A comparison was then made with a self-complementary DNA duplex $d(CGCAAATTTGCG)_2$ well-known for Hoechst 33258 affinity (*49*). UV melting of this DNA duplex with NH2 showed an effect similar to that of Hoechst 33258,

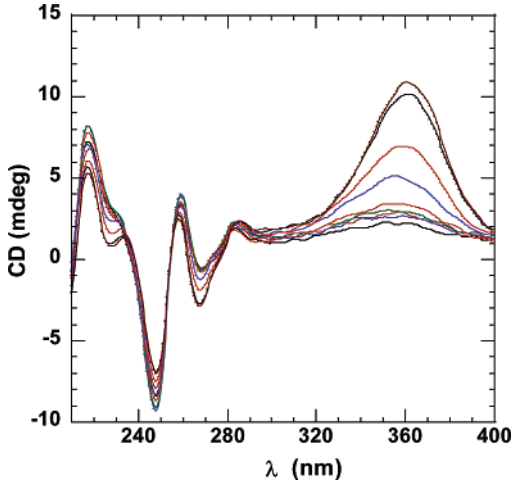

FIGURE 8: CD scans of poly(dA)·poly(dT) with increasing concentrations of Hoechst 33258. Samples of DNA (40 μM) were scanned from 400 to 210 nm after serial additions of concentrated ligand with stirring. Peaks around 360 nm correspond to induced CD of Hoechst 33258. Buffer consisted of 10 mM sodium cacodylate, 0.5 mM EDTA, and 150 mM KCl (pH 7.2) at 20 °C.

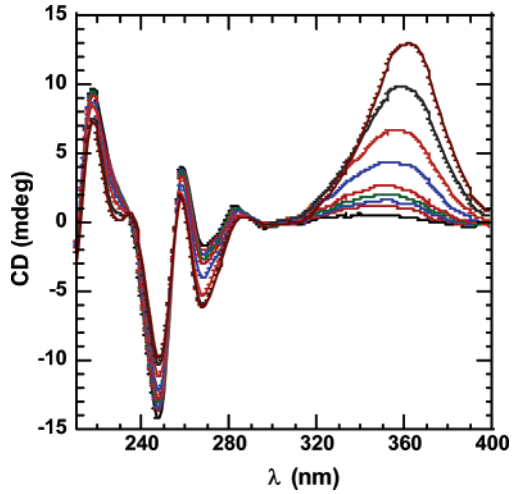

FIGURE 9: CD scans of poly(dA)·poly(dT) with increasing concentrations of NH1. Samples of DNA (40 μM) were scanned from 400 to 210 nm after serial additions of concentrated ligand with stirring. Peaks around 360 nm correspond to induced CD of Hoechst 33258. Buffer consisted of 10 mM sodium cacodylate, 0.5 mM EDTA, and 150 mM KCl (pH 7.2) at 20 °C.

with a ΔT_m of 14 °C (Figure 7), much weaker than that with NH1 (ΔT_m = 25 °C; Figure 7). The observed melting for the 12mer duplex was in excellent agreement with that reported previously (*49*).

Circular Dichroism of Poly(dA)·Poly(dT) in the Presence of NH1 and NH2 Indicates Similar Modes of Binding to Hoechst 33258. CD spectroscopy was utilized to study any changes in the poly(dA)·poly(dT) structure as well as in the Hoechst moiety of the conjugate. Numerous reports have explained DNA binding-induced chirality of Hoechst 33258, typically indicated by a change in the CD signal at the λ_{max} of Hoechst 33258 UV absorbance (*50*, *51*). In these studies, titrations of ligand into a solution of DNA were carried out, and the solutions were allowed to equilibriate before CD scans of the solution were recorded. The resulting scans were overlaid to compare the CD spectra at different ligand:DNA ratios (Figures 8−10). A significant change occurred in the CD signal in the poly(dA)·poly(dT) region, which was

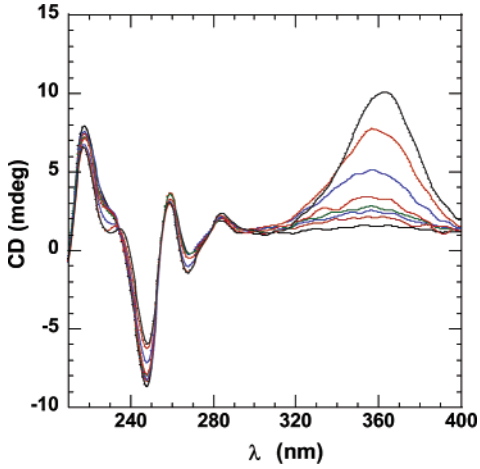

FIGURE 10: CD scans of poly(dA)·poly(dT) with increasing concentrations of NH2. Samples of DNA (40 μM) were scanned from 400 to 210 nm after serial additions of concentrated ligand with stirring. Peaks around 360 nm correspond to induced CD of Hoechst 33258. Buffer consisted of 10 mM sodium cacodylate, 0.5 mM EDTA, and 150 mM KCl (pH 7.2) at 20 °C.

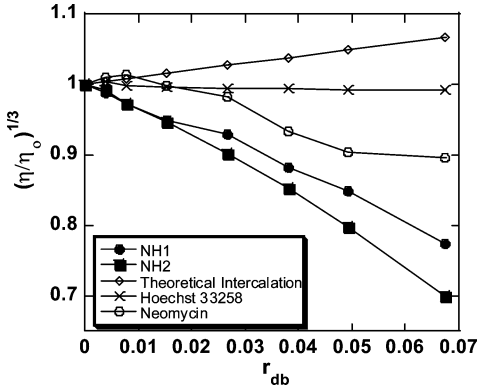

FIGURE 11: Viscometric analysis of poly(dA)·poly(dT) with various ligands. DNA solutions (100 μM) were titrated with the respective drug (200 μM), and corresponding flow times were recorded in triplicate with a deviation of <0.1 s. Buffer consisted of 10 mM sodium cacodylate, 0.5 mM EDTA, 150 mM KCl, and 1 mM $MgCl_2$ (pH 7.2) at 27 ± 0.05 °C. The *x*-axis (r_{db}) represents the molar ratio of ligand to DNA (base pairs).

represented by a negative band at 248 nm and a positive band at 260 nm. In the region of 360 nm, we also noticed an increasingly positive CD signal as ligand:DNA ratios were increased, indicative of Hoechst complexation with the DNA. In all cases (Hoechst 33258, NH1, and NH2), we observed signals corresponding to Hoechst complexation. The similar change in all three spectra suggests a similar binding mode of Hoechst in all cases.

Viscometric Titrations Suggest Neomycin Groove Binding. The experimental results gathered at this point led to consideration of a dual recognition process for NH1. Binding of neomycin in NH2 was yet unsubstantiated, primarily due to weak effects on DNA stability compared to Hoechst 33258. Circular dichroism results (Figures 9 and 10) clearly indicate Hoechst binding in both NH1 and NH2. UV melting experiments (Figures 3−7) attest to neomycin's role in binding by shifting T_m values for both polymeric and oligomeric DNA duplexes (NH1 only). For further confirmation of neomycin's role in binding of NH1 and NH2 to DNA, viscometric titrations with poly(dA)·poly(dT) were performed.

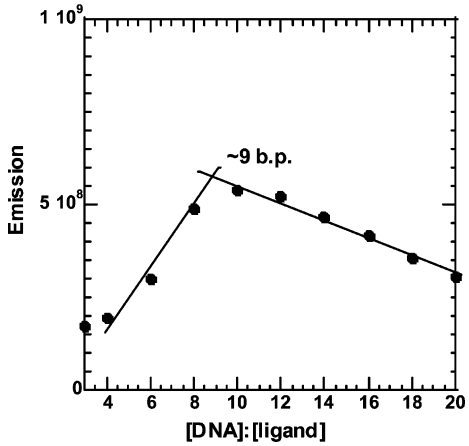

FIGURE 12: Fluorescence titration of NH1 into poly(dA)·poly(dT). Small aliquots of concentrated ligand were added to DNA (2 μM) before fluorescence analysis (excitation at 345 nm, emission scanning from 370 to 600 nm at 1 nm/s; 4 nm slit width; $T = 25$ °C). Buffer consisted of 10 mM sodium cacodylate, 0.5 mM EDTA, and 150 mM KCl (pH 7.2).

Viscometry has long been utilized for investigating ligand−substrate binding modes, particularly to confirm intercalation events. Intercalation of nucleic acids results in an increase in the helical length, because of space displacement between the base pairs by the ligand. Nucleic acids of appropriate lengths are rodlike, so an increase in helical length results in an increase in solution viscosity (*52*). Conversely, groove binding by ligands can often result in a decrease in solution viscosity, thought to be due to helical compaction (*29*, *53*). Neomycin and other aminoglycosides have been shown to elicit decreases in solution viscosity (*29*, *53*); therefore, it was fitting to corroborate dual groove binding in NH1 and NH2 using viscometry.

Viscometric titrations of various ligands with poly(dA)·poly(dT) were also carried out (Figure 11). Experiments were carried out at low r_{db} values (ratio of drug:DNA base pairs) and in the presence of Mg^{2+} to avoid DNA precipitation, which occurred at higher ligand concentrations in the absence of Mg^{2+}. For both NH1 and NH2, a considerable decrease in DNA solution viscosity was observed as ligand concentrations increased. Control experiments were also carried out using neomycin and Hoechst 33258. DNA solutions titrated with neomycin indicated slight viscosity decreases at higher ligand concentrations. Experiments with Hoechst 33258 indicated little change. Therefore, the decrease observed with both NH1 and NH2 can be attributed to the effect of neomycin in compacting the DNA duplex structure. Surprisingly, however, NH2 leads to a larger decrease in solution viscosity when compared to that with NH1 or Hoechst 33258.

Equilibrium Fluorescence Titrations Indicate Significant Enhancement of Poly(dA)·Poly(dT) Binding by NH1 over NH2 and Hoechst 33258. To further validate the binding of neomycin to duplex DNA, fluorescence was used in titrations of the ligands with poly(dA)·poly(dT) with the intent of establishing reliable association constants. To achieve this aim, an established procedure that circumvents the fluorescence effects associated with alternative modes of binding by Hoechst was utilized. Hoechst 33258 exhibits multiple modes of binding, from sequence-mediated binding (one molecule per five A·T base pair stretches) to aggregated ligand complexes (up to six molecules per five A·T base pair stretches) (*54*). Such multiple binding modes result in complex fluorescence binding relationships and therefore complicate the mathematical fitting to a theoretical binding model. To thwart these complex stoichiometries and weaken their effect on Hoechst fluorescence, Loontiens et al. established reliable binding constants, for binding of Hoechst 33258 to polymeric DNA, through fluorescence analysis of low ligand:DNA ratios (*54*−*56*). More complex interactions were avoided. As a result, the changes in fluorescence now represented the primary, high-affinity, and sequence-mediated interactions. With ligand:DNA stoichiometries now known, an independent site model can be used to similarly fit data to that previously reported. By titrating concentrated ligand solutions into DNA and monitoring changes in fluorescence, we determined stoichiometries of nine base pairs to one ligand for both NH1 and NH2 (Figure 12; see the Supporting Information for NH2 binding site size) (*57*). NH2 exhibits a much smaller change in fluorescence than NH1. The differ-

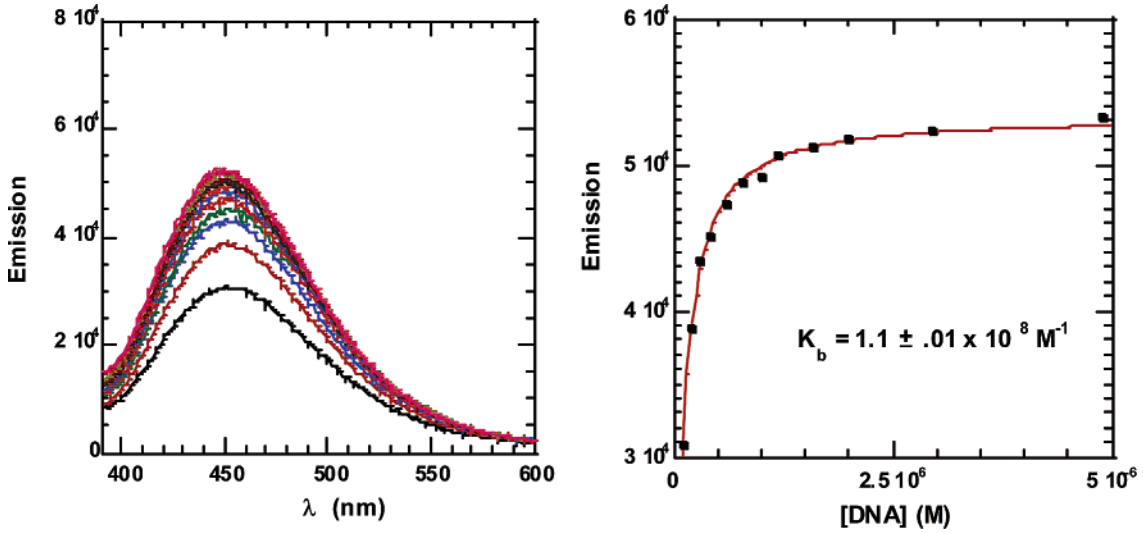

FIGURE 13: Fluorescence-detected binding of poly(dA)·poly(dT) with Hoechst 33258. Small aliquots (1−20 μL) of DNA (200 μM/bp) were added to a solution of ligand (2 mL of a 10 nM solution) before fluorescence analysis (excitation at 338 nm, emission scanning from 390 to 600 nm at 1 nm/s; 4 nm slit width; $T = 25$ °C). Buffer consisted of 10 mM sodium cacodylate, 0.5 mM EDTA, and 150 mM KCl (pH 7.2).

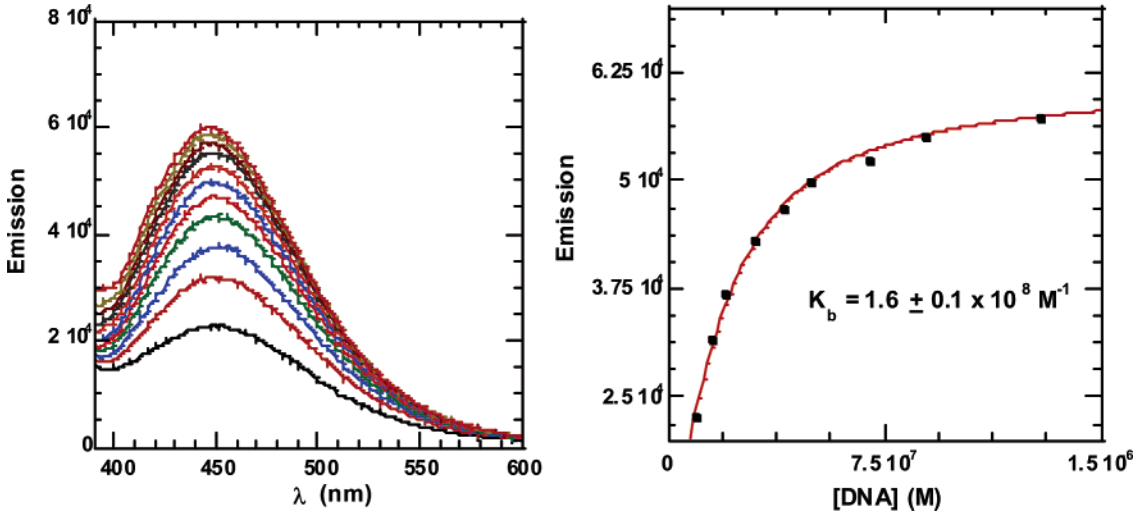

FIGURE 14: Fluorescence-detected binding of poly(dA)·poly(dT) with NH1. Small aliquots (1−20 μL) of DNA (200 μM/bp) were added to a solution of ligand (2 mL of a 10 nM solution) before fluorescence analysis (excitation at 338 nm, emission scanning from 390 to 600 nm at 1 nm/s; 4 nm slit width; T = 25 °C). Buffer consisted of 10 mM sodium cacodylate, 0.5 mM EDTA, and 150 mM KCl (pH 7.2).

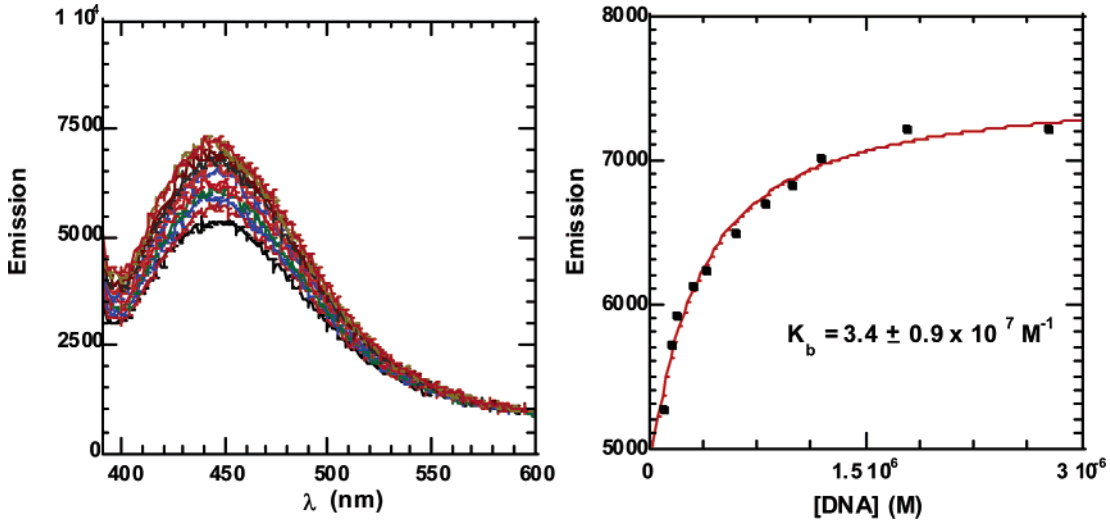

FIGURE 15: Fluorescence-detected binding of poly(dA)·poly(dT) with NH2. Small aliquots (1−20 μL) of DNA (200 μM/bp) were added to a solution of ligand (2 mL of a 10 nM solution) before fluorescence analysis (excitation at 338 nm, emission scanning from 390 to 600 nm at 1 nm/s; 4 nm slit width; T = 25 °C). Buffer consisted of 10 mM sodium cacodylate, 0.5 mM EDTA, and 150 mM KCl (pH 7.2).

ences in fluorescence at high ligand concentrations also show the binding differences between the two conjugates. Fluorescence is quenched at high NH1 concentrations, as with Hoechst 33258. This quenching is the result of free Hoechst binding to bound Hoechst. However, NH2 fluorescence at high NH2 concentrations gradually increases, which is evidence of weaker binding by this conjugate. Due to charge repulsion between the protonated Hoechst 33258 and multiprotonated neomycin, neomycin's freedom outside of the groove may prohibit unbound Hoechst 33258 from entering to bind bound Hoechst 33258.

Figures 13−15 show the results from fluorescence experiments with poly(dA)·poly(dT). A significant enhancement in fluorescence is observed for both Hoechst 33258 and NH1. However, there is a marked decrease in the fluorescence change for NH2, due to reasons described above. The observed binding constant for NH1 ($K_b = 1.6 \times 10^8$ M^{-1}) was found to be slightly higher than that for Hoechst 33258 (1.1×10^8 M^{-1}, in close agreement with that observed previously) (*58*). NH2 binding data were approximately 3-fold lower than NH1 data. These results further corroborate the observed stabilization data from UV melting experiments in the NH1−NH2 comparison showing that the NH1 conjugate is clearly a stronger binding agent than NH2.

DSC Experiments Confirm both UV and Fluorescence Data for Binding of NH1 to Poly(dA)·Poly(dT). DSC was used to further study binding of NH1 to poly(dA)·poly(dT). Using a previously described method (*59*), values for ΔH and T_m in the DNA melting process in the presence and absence of ligand were obtained (Figure 16). Values for T_m in the presence and absence of ligand (NH1) were consistent in both UV melting and DSC experiments. Values from the integrated melting transitions, along with T_m values, can be used in determining K values at any temperature. The transformation of K_{T_m} values to K at any temperature assumes a negligible ΔC_p. Though Hoechst compounds can exhibit negative ΔC_p values for DNA binding, efforts in using ITC to determine reliable ΔH values were unsuccessful due to a combination of extensive ligand aggregation and weak binding signal (even with DNA concentrations up to 100 μM). Nonetheless, DSC-derived values for K were determined at 25 °C (the temperature at which isothermal

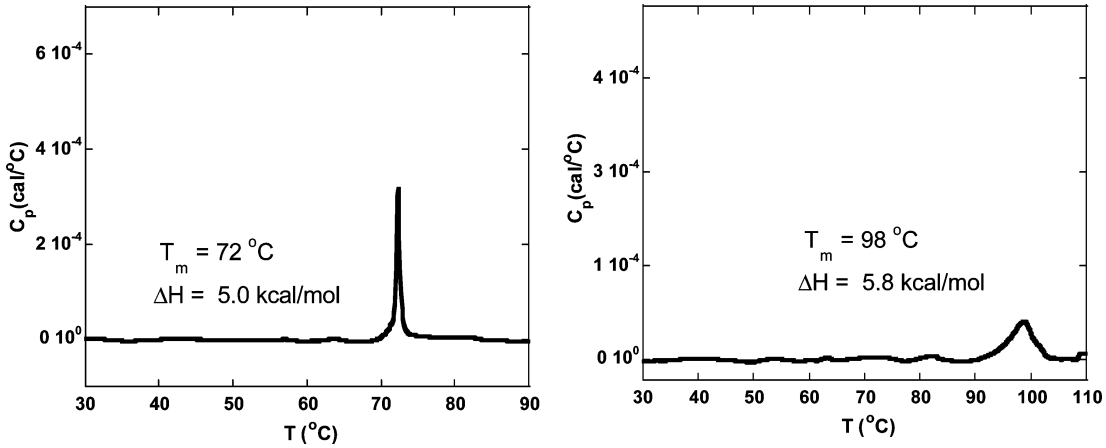

FIGURE 16: DSC profiles of 100 μM poly(dA)·poly(dT) alone (left) and in the presence of 8 μM NH1 (right). Buffer conditions were identical to those in UV melting experiments. Samples were heated at a rate of 0.5 °C/min. Values for T_m and ΔH were determined using Origin 5.0 provided with the instrument (see Materials and Methods for further details).

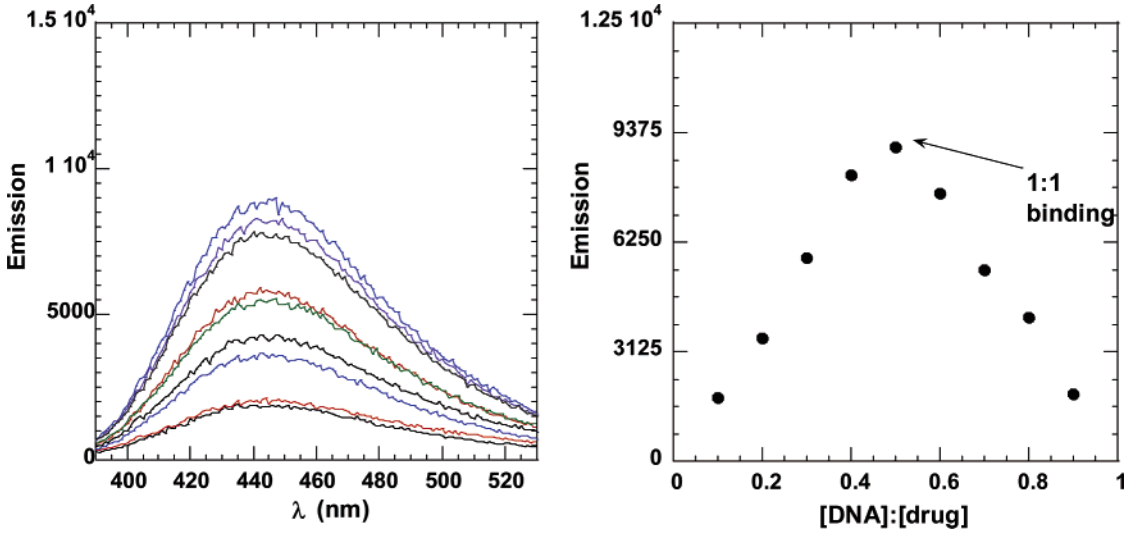

FIGURE 17: Fluorescence Job plot of Hoechst 33258 and d(CGCAAATTTGCG)$_2$. Equimolar solutions (0.9 μM) of both ligand and DNA were mixed in varying ratios and analyzed for fluorescence emission. Conditions: λ_{exc} = 338 nm, slits of 2 nm, T = 20 °C, BPES buffer [6 mM Na_2HPO_4, 2 mM NaH_2PO_4, 185 mM NaCl, and 1 mM Na_2EDTA (pH 7.0)].

fluorescence titrations were carried out). K values relied on ΔH for duplex melting alone (5.0 kcal/mol) and in the presence of saturating ligand (5.8 kcal/mol), along with T_m values in the absence (72 °C) and presence of ligand (98 °C). Using eqs 2−4 (see Methods), a value of 2.96×10^8 M^{-1} was found. This value closely agreed with the value determined from fluorescence [$(1.6 \pm 0.1) \times 10^8$ M^{-1}; see Table 1].

Equilibrium Fluorescence Titrations Indicate Significant Binding of d(CGCAAATTTGCG)$_2$ by NH1 over NH2. Figure 12 indicates that nine A·T base pairs are occupied when bound by NH1 or NH2. It was then of interest to explore the consequences of a diminished stretch of A·T bases. Therefore, d(CGCAAATTTGCG)$_2$ was chosen. The molecular modeling studies in Figure 2 clearly illustrate the potential for multiple interactions between the neomycin−Hoechst 33258 conjugates and d(CGCAAATTTGCG)$_2$. UV melting studies also clearly indicate that neomycin plays an additional role in stabilizing the duplex. Whereas NH1 stabilizes the DNA at a temperature 11 °C higher than that at which Hoechst 33258 does, NH2 is less effective. It was then necessary to further study the binding using isothermal fluorescence binding titrations.

Table 1: Binding Data for Ligands Studied[a]

conjugate	K ($\times 10^7$ M^{-1}) poly(dA)·poly(dT)	A_3T_3	N
Hoechst 33258	11 ± 1.0	18 ± 5.0	10
NH1	16 ± 1.0	3.6 ± 0.7	16
NH2	3.4 ± 0.9	0.5 ± 0.3	16

[a] Values for K_b were determined by nonlinear curve fitting of fluorescence titrations according to an independent site model using conditions similar to those reported. Values for N (binding site size) were either used as reported (Hoechst 33258) or determined experimentally.

Fluorescence titrations of d(CGCAAATTTGCG)$_2$ with Hoechst 33258, NH1, and NH2 were carried out in a fashion similar to that reported previously. This duplex maintains the central A_3T_3 region to which Hoechst 33258 is known to bind in a 1:1 fashion. With mixing curves (Job plots), where different ligand to DNA concentration ratios were monitored by fluorescence, breaks at the 50:50 ratio indicate a 1:1 stoichiometry of binding by Hoechst 33258 and the conjugates (Figures 17 and 18). In obtaining the binding isotherms, we analyzed individual samples of varying ligand:DNA ratios but with a constant ligand concentration for

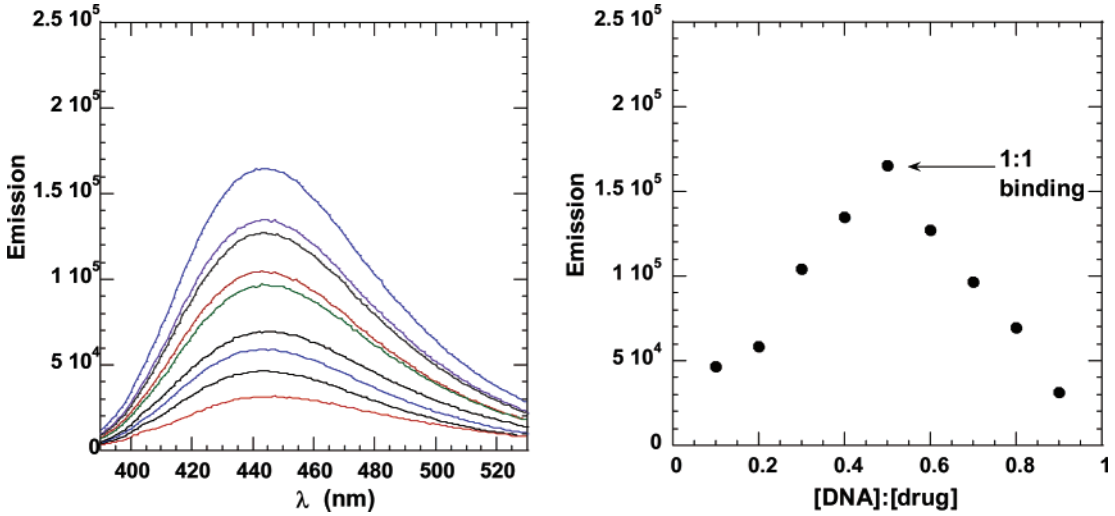

FIGURE 18: Fluorescence Job plot of NH1 and d(CGCAAATTTGCG)$_2$. Equimolar solutions (0.9 μM) of both ligand and DNA were mixed in varying ratios and analyzed for fluorescence emission. Conditions: λ_{exc} = 338 nm, slits of 2 nm, T = 20 °C, BPES buffer [6 mM Na_2HPO_4, 2 mM NaH_2PO_4, 185 mM NaCl, and 1 mM Na_2EDTA (pH 7.0)].

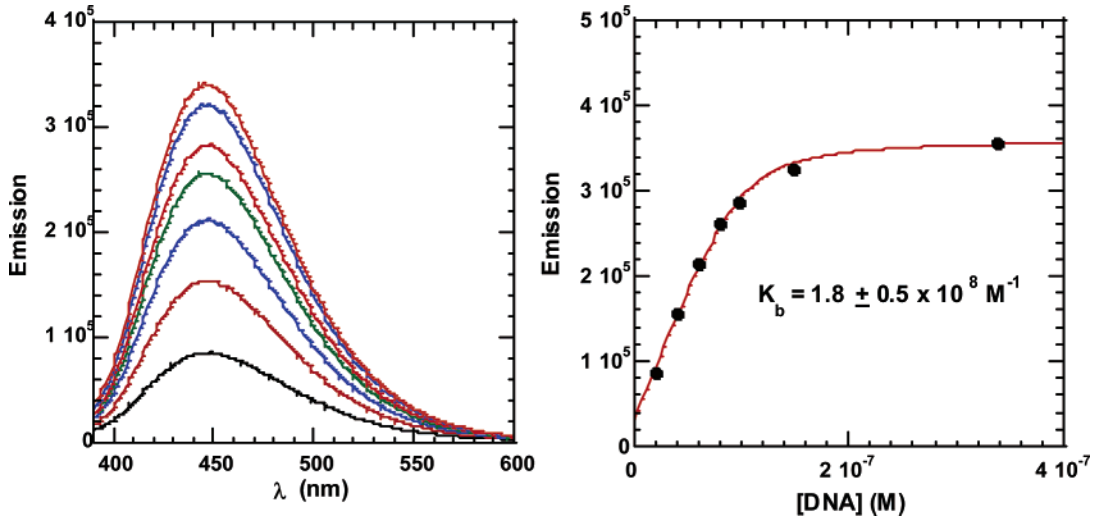

FIGURE 19: Fluorescence-detected binding of d(CGCAAATTTGCG)$_2$ with Hoechst 33258. Individual samples of ligand (100 nM in 2 mL) mixed with varying concentrations of DNA were prepared immediately after quantitation of both stock ligand and DNA solutions. After sufficient mixing of solutions and equilibration (30 min), each sample was analyzed for fluorescence emission over the 390−600 nm range. Conditions: λ_{exc} = 338 nm, slits of 4 nm, T = 20 °C, BPES buffer [6 mM Na_2HPO_4, 2 mM NaH_2PO_4, 185 mM NaCl, and 1 mM Na_2EDTA (pH 7.0)].

fluorescence in a fashion similar to those used for polymeric DNA. It is worth mentioning that single sample titrations, like those with polymeric DNA, gave less reliable results likely due to sample equilibration. Fluorescence scans and binding curves for both NH1 and NH2 are shown in Figures 19−21. Hoechst 33258 binding was found to be in good agreement with that reported previously. However, NH1 binding was clearly weaker than Hoechst 33258 binding (nearly 6-fold, 3.6×10^7 M^{-1}) and NH2 binding even weaker (nearly 40-fold, 5×10^6 M^{-1}). These results were quite surprising considering the aforementioned UV melting data. However, such a phenomenon has been observed recently with similar Hoechst-type molecules. Searle has shown that Hoechst analogues with the largest ΔT_m exhibit significantly lower isothermal binding constants (*60*). The underlying factor for such phenomena was linked to reports that binding of Hoechst 33258 to d(CGCAAATTTGCG)$_2$ exhibits a significant negative ΔC_p (*49*), making binding constant determinations largely temperature dependent. Modifications in features such as hydrophobic surface area may result in an increased binding affinity at elevated temperatures, where conformational changes may maximize hydrophobic effects.

Also apparent is the relationship of binding constant with DNA sequence. NH1 clearly displays stronger binding to poly(dA)·poly(dT) in both isothermal fluorescence and UV melting experiments. A contrasting relationship between T_m and K_b is obvious with d(CGCAAATTTGCG)$_2$. The likely explanation for the lower K_b for binding of NH1 to this DNA lies with the neighboring G·C base pairs that are less favorable binding domains for the neomycin−Hoechst 33258 conjugate. As depicted in Figure 11, the conjugates occupy nine A·T base pairs upon binding to poly(dA)·poly(dT); the oligomer contains three fewer A·T base pairs.

Breaking the A·T Stretch: NH1 Also Stabilizes A_2GCT_2 Stretches of DNA, whereas Hoechst 33258 Shows No Effect. To investigate the sequence specificity of conjugates, it was necessary to probe the affinity of Hoechst 33258, and NH1 and NH2 for sequences in which a G·C junction interrupts

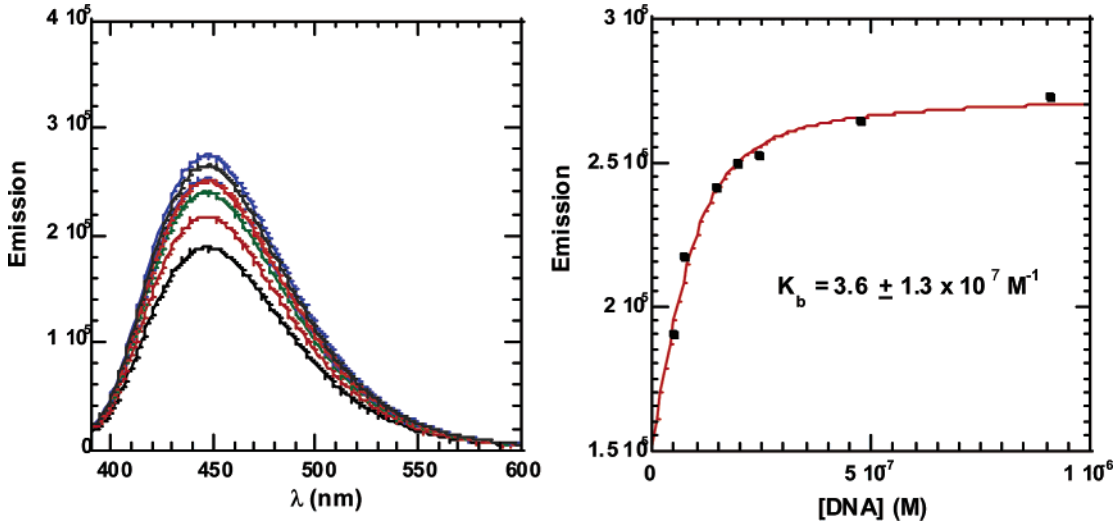

FIGURE 20: Fluorescence-detected binding of d(CGCAAATTTGCG)$_2$ with NH1. Individual samples of ligand (100 nM in 2 mL) mixed with varying concentrations of DNA were prepared immediately after quantitation of both stock ligand and DNA solutions. After sufficient mixing of solutions and equilibration (30 min), each sample was analyzed for fluorescence emission over the 390−600 nm range. Conditions: $\lambda_{exc} = 338$ nm, slits of 4 nm, $T = 20$ °C, BPES buffer [6 mM Na_2HPO_4, 2 mM NaH_2PO_4, 185 mM NaCl, and 1 mM Na_2EDTA (pH 7.0)].

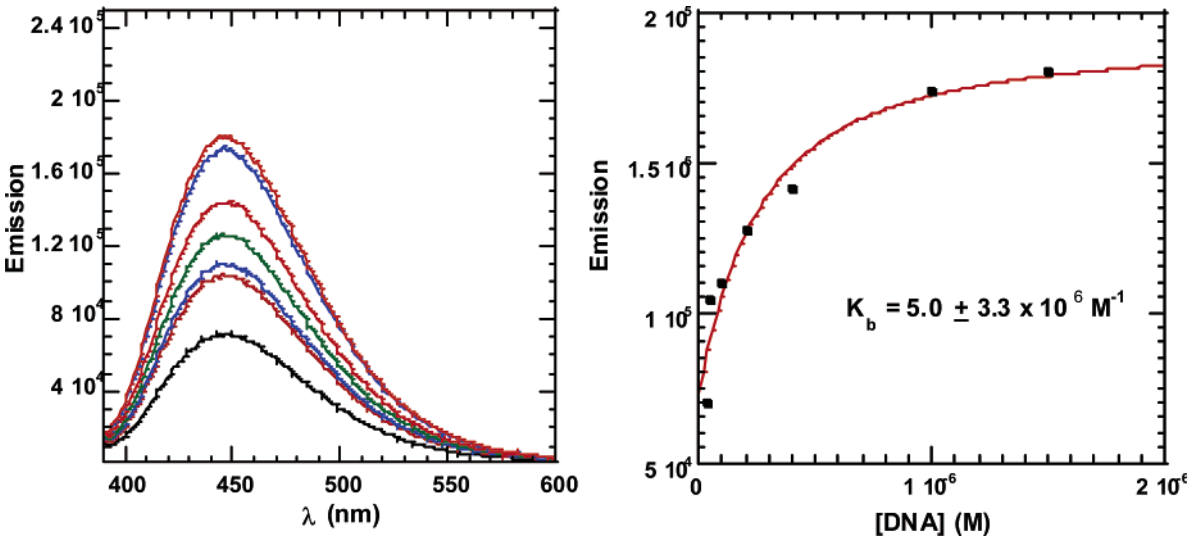

FIGURE 21: Fluorescence-detected binding of d(CGCAAATTTGCG)$_2$ with NH2. Individual samples of ligand (100 nM in 2 mL) mixed with varying concentrations of DNA were prepared immediately after quantitation of both stock ligand and DNA solutions. After sufficient mixing of solutions and equilibration (30 min), each sample was analyzed for fluorescence emission over the 390−600 nm range. Conditions: $\lambda_{exc} = 338$ nm, slits of 4 nm, $T = 20$ °C, BPES buffer [6 mM Na_2HPO_4, 2 mM NaH_2PO_4, 185 mM NaCl, and 1 mM Na_2EDTA (pH 7.0)].

the A_nT_n stretch. Hoechst 33258 has been shown to bind A·T stretches from four to six base pairs in length. Introduction of G·C base pairs has also been shown to significantly weaken the binding of Hoechst 33258. Therefore, studying a sequence with a G·C junction can provide deeper insight into neomycin's role in binding. For example, does binding by neomycin perturb the sequence specificity of Hoechst? Therefore, a study using DNA duplex d(CGCAA**GC**TTGCG)$_2$ was undertaken.

Fluorescence titration experiments with d(CGCAA**GC**TTGCG)$_2$, Hoechst 33258, and NH1 were carried out like the experiments with the central A_3T_3 stretch. In both cases, the observed K_b values were very similar but significantly lower than what was observed for d(CGCAAATTTGCG)$_2$. The binding is nearly 1000-fold weaker for both Hoechst 33258 and NH1 (Figure 22), validating previous accounts which indicated a strong binding preference of Hoechst ligands for A_nT_n regions of DNA. NH1 has a lower affinity [$K_b = (1.5 \pm 0.2) \times 10^5$ M^{-1}] than Hoechst 33258 [$K_b = (3.7 \pm 0.3) \times 10^5$ M^{-1}].

UV melting experiments provided similar results with Hoechst 33258. Whereas Hoechst 33258 had no effect on the T_m of the duplex, NH1 exhibited a slight stabilization of this duplex, with a T_m 5 °C higher than that observed in the absence of ligand (Figure 23). Neomycin's role in stabilization of G·C rich sequences can be attributed to its propensity for A-form structures (G·C rich sequences are known to adopt A-form structures, whereas A·T rich sequences maintain the B-form). Therefore, neomycin plays a clear role in stabilization of d(CGCAA**GC**TTGCG)$_2$, as well as the A_3T_3 analogue given the high ΔT_m versus Hoechst 33258. These results also support previous results which showed that the binding constant and ΔT_m data cannot always be correlated. NH1 clearly exhibits stabilization of d(CG-

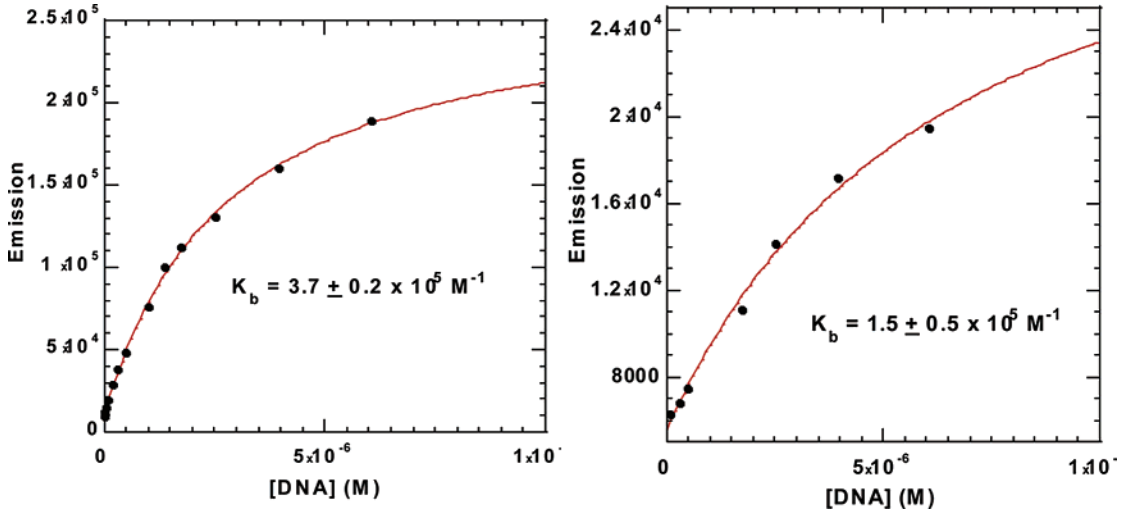

FIGURE 22: Fluorescence-detected binding curves for binding of d(CGCAA**GC**TTGCG)$_2$ to Hoechst 33258 (left) and NH1 (right). Individual samples of ligand (100 nM in 2 mL) mixed with varying concentrations of DNA were prepared immediately after quantitation of both stock ligand and DNA solutions. After sufficient mixing of solutions and equilibration (30 min), each sample was analyzed for fluorescence emission over the 390−600 nm range. Conditions: λ_{exc} = 338 nm, slits of 4 nm, T = 20 °C, BPES buffer [6 mM Na_2HPO_4, 2 mM NaH_2PO_4, 185 mM NaCl, and 1 mM Na_2EDTA (pH 7.0)].

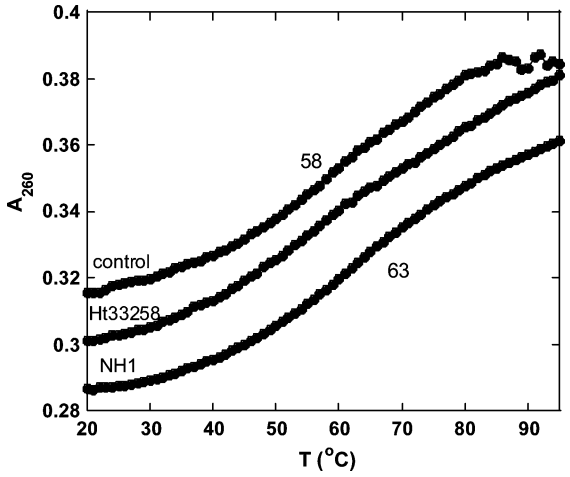

FIGURE 23: UV melting profiles of d(CGCAA**GC**TTGCG)$_2$ with various ligands. Samples of DNA (1 μM in duplex) were mixed with ligand (1 μM) in BPES buffer [6 mM Na_2HPO_4, 2 mM $NaHPO_4$, 1 mM EDTA, and 185 mM NaCl (pH 7.0)] before being heated at 95 °C for 5 min and slowly annealed to 20 °C before UV analysis at 260 nm from 20 to 95 °C at a heating rate of 0.2 °C/min.

CAAGCTTGCG)$_2$ in UV melting, whereas Hoechst 33258 does not. However, the observed equilibrium binding data indicate a slightly lower affinity for NH1.

CONCLUSION

A recent report indicated that neomycin specificity is for nucleic acids known to adopt the A-form. We have since endeavored to explore neomycin's utility in binding to B-DNA to gain a better understanding of the molecular forces that dictate aminoglycoside binding within the DNA major groove. From the current study of novel neomycin−Hoechst 33258 conjugates designed for probing binding of neomycin to B-DNA, the following conclusions can be drawn. (a) NH1 and NH2 were shown to significantly enhance the thermal stability of B-DNA. NH1 was found to exhibit a more significant enhancement than both NH2 and Hoechst 33258 alone. UV melting experiments with both polymeric and oligomeric DNA indicate significant shifts in T_m when compared with those of samples in the absence of ligand. (b) Triplex DNA inhibition by both NH1 and NH2 suggests dual-groove binding. UV melting experiments of NH1 and NH2 under triplex-forming conditions indicated an inhibition of TFO binding, likely due to binding of neomycin in the major groove. Furthermore, viscosity experiments indicate binding of neomycin (in NH1 and NH2) to B-DNA involves a groove binding mode. (c) The mode of binding of Hoechst to DNA is the same in all ligands that were studied. CD experiments indicate similar spectral patterns for poly(dA)·poly(dT) when titrated with either Hoechst 33258, NH1, or NH2. (d) The optimal binding site for the conjugates includes a contiguous stretch of nine A·T base pairs. Fluorescence titrations indicated base pair:ligand ratios of 9:1 for both NH1 and NH2 and a binding constant for NH1 with poly(dA)·poly(dT) higher than that of Hoechst 33258. The importance of the extended A·T base pair site for strong binding was further illustrated in studies with both shorter A·T stretches and interrupted A·T stretches. Binding of NH1 to d(CGCAAATTTGCG)$_2$ exhibited lower affinities than Hoechst 33258. For both Hoechst 33258 and NH1, K_b values decrease significantly for the A_2GCT_2 duplex versus those for the A_3T_3 duplex. (e) The linker between Hoechst and neomycin plays an important role in delivering both binding moieties to the grooves. Both UV melting and fluorescence data indicate significant enhancement of DNA binding for NH1 over NH2. Molecular modeling indicates a more constrained tandem interaction between the two moieties due to the decreased degree of freedom of the shorter pentane linker. Conjugates of different minor groove binders and linker sizes can then perhaps be designed to target a structure of preference and should aid in the development of even more selective and potent conjugates. Altogether, these results further illustrate that NH1 is not only a remarkable DNA binder but also a lead compound that can be used to better understand the molecular requirements for successful dual groove recognition of B-DNA.

SUPPORTING INFORMATION AVAILABLE

NMR scans, MALDI, and HPLC of conjugates. This material is available free of charge via the Internet at http://pubs.acs.org.

REFERENCES

1. Magnet, S., and Blanchard, J. S. (2005) Molecular Insights into Aminoglycoside Action and Resistance, *Chem. Rev. 105*, 477−497.
2. Willis, B., and Arya, D. P. (2006) An Expanding View of Aminoglycoside-Nucleic Acid Recognition, *Adv. Carbohydr. Chem. Biochem. 60*, 263−314.
3. Calnan, B. J., Tidor, B., Biancalana, S., Hudson, D., and Frankel, A. D. (1991) Arginine-mediated RNA recognition: The arginine fork, *Science 252*, 1167−1171.
4. Cordingley, M. G., LaFemina, R. L., Callahan, P. L., Condra, J. H., Sardana, V. V., Graham, D. J., Nguyen, T. M., LeGrow, K., Gotlib, L., et al. (1990) Sequence-specific interaction of Tat protein and Tat peptides with the transactivation-responsive sequence element of human immunodeficiency virus type 1 in vitro, *Proc. Natl. Acad. Sci. U.S.A. 87*, 8985−8989.
5. Edwards, T. E., and Sigurdsson, S. T. (2002) Electron Paramagnetic Resonance Dynamic Signatures of TAR RNA-Small Molecule Complexes Provide Insight into RNA Structure and Recognition, *Biochemistry 41*, 14843−14847.
6. Faber, C., Sticht, H., Schweimer, K., and Rosch, P. (2000) Structural rearrangements of HIV-1 Tat-responsive RNA upon binding of neomycin B, *J. Biol. Chem. 275*, 20660−20666.
7. Wang, S., Huber, P. W., Cui, M., Czarnik, A. W., and Mei, H.-Y. (1998) Binding of Neomycin to the TAR Element of HIV-1 RNA Induces Dissociation of Tat Protein by an Allosteric Mechanism, *Biochemistry 37*, 5549−5557.
8. Hendrix, M., Priestley, E. S., Joyce, G. F., and Wong, C.-H. (1997) Direct Observation of Aminoglycoside-RNA Interactions by Surface Plasmon Resonance, *J. Am. Chem. Soc. 119*, 3641−3648.
9. Lacourciere, K. A., Stivers, J. T., and Marino, J. P. (2000) Mechanism of Neomycin and Rev Peptide Binding to the Rev Responsive Element of HIV-1 As Determined by Fluorescence and NMR Spectroscopy, *Biochemistry 39*, 5630−5641.
10. Luedtke, N. W., and Tor, Y. (2003) Fluorescence-based methods for evaluating the RNA affinity and specificity of HIV-1 Rev-RRE inhibitors, *Biopolymers 70*, 103−119.
11. Luedtke, N. W., Liu, Q., and Tor, Y. (2003) RNA-Ligand Interactions: Affinity and Specificity of Aminoglycoside Dimers and Acridine Conjugates to the HIV-1 Rev Response Element, *Biochemistry 42*, 11391−11403.
12. Tok, J. B. H., Dunn, L. J., and Des Jean, R. C. (2001) Binding of dimeric aminoglycosides to the HIV-1 rev responsive element (RRE) RNA construct, *Bioorg. Med. Chem. Lett. 11*, 1127−1131.
13. Darlix, J. L., Gabus, C., Nugeyre, M. T., Clavel, F., and Barre-Sinoussi, F. (1990) Cis elements and trans-acting factors involved in the RNA dimerization of the human immunodeficiency virus HIV-1, *J. Mol. Biol. 216*, 689−699.
14. McPike, M. P., Goodisman, J., and Dabrowiak, J. C. (2004) Specificity of neomycin analogues bound to the packaging region of human immunodeficiency virus type 1 RNA, *Bioorg. Med. Chem. 12*, 1835−1843.
15. McPike, M. P., Sullivan, J. M., Goodisman, J., and Dabrowiak, J. C. (2002) Footprinting, circular dichroism and UV melting studies on neomycin B binding to the packaging region of human immunodeficiency virus type-1 RNA, *Nucleic Acids Res. 30*, 2825−2831.
16. Chia, J. S., Wu, H. L., Wang, H. W., Chen, D. S., and Chen, P. J. (1997) Inhibition of hepatitis delta virus genomic ribozyme self-cleavage by aminoglycosides, *J. Biomed. Sci. 4*, 208−216.
17. Rogers, J., Chang, A. H., von Ahsen, U., Schroeder, R., and Davies, J. (1996) Inhibition of the self-cleavage reaction of the human hepatitis delta virus ribozyme by antibiotics, *J. Mol. Biol. 259*, 916−925.
18. Clouet-d'Orval, B., Stage, T. K., and Uhlenbeck, O. C. (1995) Neomycin Inhibition of the Hammerhead Ribozyme Involves Ionic Interactions, *Biochemistry 34*, 11186−11190.
19. Hermann, T., and Westhof, E. (1998) Aminoglycoside binding to the hammerhead ribozyme: A general model for the interaction of cationic antibiotics with RNA, *J. Mol. Biol. 276*, 903−912.
20. Tor, Y., Hermann, T., and Westhof, E. (1998) Deciphering RNA recognition: Aminoglycoside binding to the hammerhead ribozyme, *Chem. Biol. 5*, R277−R283.
21. von Ahsen, U., Davies, J., and Schroeder, R. (1991) Antibiotic inhibition of group I ribozyme function, *Nature 353*, 368−370.
22. von Ahsen, U., and Noller, H. F. (1993) Footprinting the sites of interaction of antibiotics with catalytic group I intron RNA, *Science 260*, 1500−1503.
23. Hoch, I., Berens, C., Westhof, E., and Schroeder, R. (1998) Antibiotic inhibition of RNA catalysis: Neomycin B binds to the catalytic core of the td group I intron displacing essential metal ions, *J. Mol. Biol. 282*, 557−569.
24. Tekos, A., Tsagla, A., Stathopoulos, C., and Drainas, D. (2000) Inhibition of eukaryotic ribonuclease P activity by aminoglycosides: Kinetic studies, *FEBS Lett. 485*, 71−75.
25. Eubank, T. D., Biswas, R., Jovanovic, M., Litovchick, A., Lapidot, A., and Gopalan, V. (2002) Inhibition of bacterial RNase P by aminoglycoside-arginine conjugates, *FEBS Lett. 511*, 107−112.
26. Mikkelsen, N. E., Brannvall, M., Virtanen, A., and Kirsebom, L. A. (1999) Inhibition of RNase P RNA cleavage by aminoglycosides, *Proc. Natl. Acad. Sci. U.S.A. 96*, 6155−6160.
27. Arya, D. P., Coffee, R. L., Jr., Willis, B., and Abramovitch, A. I. (2001) Aminoglycoside-nucleic acid interactions: Remarkable stabilization of DNA and RNA triple helices by neomycin, *J. Am. Chem. Soc. 123*, 5385−5395.
28. Arya, D. P., and Coffee, R. L., Jr. (2000) DNA triple helix stabilization by aminoglycoside antibiotics, *Bioorg. Med. Chem. Lett. 10*, 1897−1899.
29. Arya, D. P., Micovic, L., Charles, I., Coffee, R. L., Jr., Willis, B., and Xue, L. (2003) Neomycin Binding to Watson-Hoogsteen (W-H) DNA Triplex Groove: A Model, *J. Am. Chem. Soc. 125*, 3733−3744.
30. Arya, D. P., Xue, L., and Tennant, P. (2003) Combining the best in triplex recognition: Synthesis and nucleic acid binding of a BQQ-neomycin conjugate, *J. Am. Chem. Soc. 125*, 8070−8071.
31. Xue, L., Charles, I., and Arya, D. P. (2002) Pyrene-neomycin conjugate: Dual recognition of a DNA triple helix, *Chem. Commun.*, 70−71.
32. Arya, D. P., Coffee, R. L., Jr., and Charles, I. (2001) Neomycin-induced hybrid triplex formation, *J. Am. Chem. Soc. 123*, 11093−11094.
33. Arya, D. P., Xue, L., and Willis, B. (2003) Aminoglycoside (Neomycin) Preference Is for A-Form Nucleic Acids, Not Just RNA: Results from a Competition Dialysis Study, *J. Am. Chem. Soc. 125*, 10148−10149.
34. Arya, D. P. (2005) Aminoglycoside-Nucleic Acid Interactions: The case for Neomycin, in *Topics in Current Chemistry: DNA Binders* (Chaires, J. B., and Waring, M. J., Eds.) Vol. 253, pp 149−178, Springer-Verlag, Heidelburg, Germany.
35. Willis, A., III, and Arya, D. P. (2006) Major Groove Recognition of DNA by Carbohydrates, *Curr. Org. Chem. 10*, 663−673.
36. Arya, D. P., Coffee, R. L., and Xue, L. (2004) From triplex to B-form duplex stabilization: Reversal of target selectivity by aminoglycoside dimers, *Bioorg. Med. Chem. Lett. 14*, 4643−4646.
37. Frau, S., Bernadou, J., and Meunier, B. (1997) Nuclease Activity and Binding Characteristics of a Cationic "Manganese Porphyrin-Bis(benzimidazole) Dye (Hoechst 33258)" Conjugate, *Bioconjugate Chem. 8*, 222−231.
38. Frau, S., Bichenkova, E. V., Morris, G. A., and Douglas, K. T. (2001) Binding of a porphyrin conjugate of Hoechst 33258 to DNA. II. NMR spectroscopic studies detect multiple binding modes to a 12-mer nonself-complementary duplex DNA, *Nucleosides, Nucleotides Nucleic Acids 20*, 145−156.
39. Satz, A. L., and Bruice, T. C. (2002) Recognition of nine base pair sequences in the minor groove of DNA at subpicomolar concentrations by a novel microgonotropen, *Bioorg. Med. Chem. 10*, 241−252.
40. Satz, A. L., and Bruice, T. C. (2001) Recognition of nine base pairs in the minor groove of DNA by a tripyrrole peptide-Hoechst conjugate, *J. Am. Chem. Soc. 123*, 2469−2477.
41. Satz, A. L., and Bruice, T. C. (2000) Synthesis of fluorescent microgonotropens (FMGTs) and their interactions with dsDNA, *Bioorg. Med. Chem. Lett. 8*, 1871−1880.
42. Satz, A. L., and Bruice, T. C. (1999) Synthesis of a fluorescent microgonotropen (FMGT-1) and its interactions with the dodecamer d(CCGGAATTCCGG), *Bioorg. Med. Chem. Lett. 9*, 3261−3266.

43. Wiederholt, K., and McLaughlin, L. W. (1998) Duplex stabilization by DNA-hoechst 33258 conjugates: Effects of base pair mismatches, *Nucleosides Nucleotides 17*, 1895−1904.
44. Wiederholt, K., Rajur, S. B., Giuliano, J., Jr., O'Donnell, M. J., and McLaughlin, L. W. (1996) DNA-Tethered Hoechst Groove-Binding Agents: Duplex Stabilization and Fluorescence Characteristics, *J. Am. Chem. Soc. 118*, 7055−7062.
45. Rajur, S. B., Robles, J., Wiederholt, K., Kuimelis, R. G., and McLaughlin, L. W. (1997) Hoechst 33258 Tethered by a Hexa(ethyleneglycol) Linker to the 5′-Termini of Oligodeoxynucleotide 15-Mers: Duplex Stabilization and Fluorescence Properties, *J. Org. Chem. 62*, 523−529.
46. Robles, J., and McLaughlin, L. W. (1997) DNA Triplex Stabilization Using a Tethered Minor Groove Binding Hoechst 33258 Analog, *J. Am. Chem. Soc. 119*, 6014−6021.
47. Arya, D. P., and Willis, B. (2003) Reaching into the major groove of B-DNA: Synthesis and nucleic acid binding of a neomycin-Hoechst 33258 conjugate, *J. Am. Chem. Soc. 125*, 12398−12399.
48. Arya, D. P., and Willis, B. (2003) Reaching into the major groove of B-DNA: Synthesis and nucleic acid binding of a neomycin-Hoechst 33258 conjugate, *J. Am. Chem. Soc. 125*, 12398−12399.
49. Haq, I., Ladbury, J. E., Chowdhry, B. Z., Jenkins, T. C., and Chaires, J. B. (1997) Specific binding of Hoechst 33258 to the d(CGCAAATTTGCG)$_2$ duplex: Calorimetric and spectroscopic studies, *J. Mol. Biol. 271*, 244−257.
50. Rao, K. E., and Lown, J. W. (1991) Molecular recognition between ligands and nucleic acids: DNA binding characteristics of analogs of Hoechst 33258 designed to exhibit altered base and sequence recognition, *Chem. Res. Toxicol. 4*, 661−669.
51. Canzonetta, C., Caneva, R., Savino, M., Scipioni, A., Catalanotti, B., and Galeone, A. (2002) Circular dichroism and thermal melting differentiation of Hoechst 33258 binding to the curved (A_4T_4) and straight (T_4A_4) DNA sequences, *Biochim. Biophys. Acta 1576*, 136−142.
52. Cohen, G., and Eisenberg, H. (1969) Viscosity and sedimentation study of sonicated DNA-proflavine complexes, *Biopolymers 8*, 45−55.
53. Jin, E., Katritch, V., Olson, W. K., Kharatisvili, M., Abagyan, R., and Pilch, D. S. (2000) Aminoglycoside Binding in the Major Groove of Duplex RNA: The Thermodynamic and Electrostatic Forces that Govern Recognition, *J. Mol. Biol. 298*, 95−110.
54. Loontiens, F. G., Regenfuss, P., Zechel, A., Dumortier, L., and Clegg, R. M. (1990) Binding characteristics of Hoechst 33258 with calf thymus DNA, poly[d(A-T)] and d(CCGGAATTCCGG): Multiple stoichiometries and determination of tight binding with a wide spectrum of site affinities, *Biochemistry 29*, 9029−9039.
55. Breusegem, S. Y., Sadat-Ebrahimi, S. E., Douglas, K. T., Clegg, R. M., and Loontiens, F. G. (2001) Increased Stability and Lifetime of the Complex Formed between DNA and meta-Phenyl-substituted Hoechst Dyes as Studied by Fluorescence Titrations and Stopped-flow Kinetics, *J. Mol. Biol. 308*, 649−663.
56. Breusegem, S. Y., Sadat-Ebrahimi, S. E., Douglas, K. T., Bichenkova, E. V., Clegg, R. M., and Loontiens, F. G. (2001) Experimental precedent for the need to involve the primary hydration layer of DNA in lead drug design, *J. Med. Chem. 44*, 2503−2506.
57. Eftink, M. R. (1997) Fluorescence methods for studying equilibrium macromolecule-ligand interactions, *Methods Enzymol. 278*, 221−257.
58. Haq, I., Ladbury, J. E., Chowdhry, B. Z., Jenkins, T. C., and Chaires, J. B. (1997) Specific Binding of Hoechst 33258 to the d(CGCAAATTTGCG)$_2$ duplex: Calorimetric and Spectroscopic Studies, *J. Mol. Biol. 271*, 244−257.
59. Leng, F., Priebe, W., and Chaires, J. B. (1998) Ultratight DNA Binding of a New Bisintercalating Anthracycline Antibiotic, *Biochemistry 37*, 1743−1753.
60. Bostock-Smith, C. E., and Searle, M. S. (1999) DNA minor groove recognition by bis-benzimidazole analogs of Hoechst 33258: Insights into structure-DNA affinity relationships assessed by fluorescence titration measurements, *Nucleic Acids Res. 27*, 1619−1624.

BI0609265